

# Artificial Intelligence in Tumor Subregion Analysis Based on Medical Imaging: A Review

Mingquan Lin, Jacob Wynne, Yang Lei, Tonghe Wang, Walter J. Curran, Tian Liu and Xiaofeng Yang\*  
Department of Radiation Oncology and Winship Cancer Institute, Emory University, Atlanta, GA 30322

## \*Corresponding author:

Xiaofeng Yang, PhD  
Department of Radiation Oncology  
Emory University School of Medicine  
1365 Clifton Road NE  
Atlanta, GA 30322  
E-mail: xiaofeng.yang@emory.edu

## Abstract

Medical imaging is widely used in cancer diagnosis and treatment, and artificial intelligence (AI) has achieved tremendous success in various tasks of medical image analysis. This paper reviews AI-based tumor subregion analysis in medical imaging. We summarize the latest AI-based methods for tumor subregion analysis and their applications. Specifically, we categorize the AI-based methods by training strategy: supervised and unsupervised. A detailed review of each category is presented, highlighting important contributions and achievements. Specific challenges and potential AI applications in tumor subregion analysis are discussed.

**keywords:** Artificial intelligence (AI), Machine learning (ML), Deep learning (DL), Tumor subregion, Medical imaging

## 1 INTRODUCTION

In current clinical practice and research, tumor is usually assumed to be homogeneous or heterogeneous with similar distribution throughout the entire volume [2, 26, 49, 59, 153]. Recent studies have shown that some tumor regions may be more biologically aggressive than others and may play a dominant role in disease progression [41, 53, 109]. Neglecting such tumor heterogeneity at various spatial and temporal scales can lead to failures in prognosis and treatment [53]. Medical imaging has been shown to be able to reveal and quantify the heterogeneity within tumors [54, 116, 118]. Individual tumor can then be divided into sub-regions based on detected regional variations. Diagnosis, prognosis, and evaluation of treatment response can be performed individually in these subregions, and has proved superior to a simple analysis of the whole tumor [6, 38]. Therefore, accurate detection and analysis of tumor sub-regions is of great clinical and research interest.

Over the last few years, artificial intelligence (AI) has achieved tremendous success in various tasks in the field of medical imaging [23, 35, 33, 34, 52, 57, 86, 93, 94]. Many AI-based methods have been proposed to locate and analyse tumor subregions for a variety of imaging modalities and clinical tasks. In this study, we review the applications of supervised and unsupervised AI models in imaging-based tumor subregion analysis. With this survey, we aim to:

1. Summarize the latest developments of AI applications in imaging-based tumor subregion analysis.
2. Highlight contributions, identify challenges, and outline future trends.

## 2 ARTIFICIAL INTELLIGENCE

AI is a field that seeks to enable machines to learn from experience, think like humans, and perform human-like tasks. Machine learning (ML) is a discipline within AI, in which computers are trained to automatically improve performance on specific tasks based on experience. Training methods in ML are broadly composed of supervised, semi-supervised, or unsupervised strategies, each with decreasing need for human input. Within ML, deep learning (DL) employs multi-layer (“deep”) networks of mathematical functions initially intended to imitate the structure and function of the human brain to fundamentally create a mapping from one representational domain to another (e.g. categorizing photos to names of the objects they contain). Both supervised and unsupervised methods are commonly used in DL for medical image analysis.

### 2.1 Supervised learning

In supervised learning, an algorithm is designed to learn a mapping function  $f(\bullet)$  from the input variable ( $x$ ) to the output variable ( $Y$ ), i.e.  $Y=f(x)$ . The goal is to approximate the mapping function well so that the output variable ( $Y$ ) of new input data ( $x$ ) can be accurately predicted. Least-absolute-shrinkage-and-selection-operator (Lasso), random forest (RF), support vector machine (SVM), and artificial neural networks (ANN) are widely used algorithms in determining the mapping function. The Lasso is a shrinkage and feature selection method for linear regression [138]. It minimizes the sum of squared errors and the sum of the absolute value of coefficients. RF is an ensemble learning algorithm that boosts performance by combining the results of many weaker algorithms effectively reducing overfitting and building a model that is robust for discrete values in the feature space [90]. The object of SVM is to find a hyperplane in  $n$ -dimensional space that maximizes the separation of different classes of data in the feature space [19].

The multilayer perceptron (MLP) is a class of feedforward ANN wherein the biological unit of the brain, the neuron, is modeled by the mathematical unit of a network node [126]. An MLP consists of at least three layers of nodes: an input layer, hidden layer, and output layer. All nodes except the inputs employ nonlinear activation functions. MLP uses a supervised learning technique called backpropagation to update the parameters of each node. The multilayer structure and nonlinear activation of MLP distinguish it from linear perceptrons and allow it to distinguish data that are not linearly separable. Although MLP has been successfully applied to practical problems in many fields, these models must be carefully trained and thoughtfully deployed to avoid overfitting or, alternatively, failure of convergence during inference.

Convolutional neural networks (CNN) have been widely applied in many tasks [5, 50, 55, 82, 137, 166, 167, 170]. A typical CNN may be composed of several layers performing discrete computational tasks including: convolution at various scales of resolution, maximum or other forms of pooling, and batch normalization. The outputs of these layers may be omitted as in dropout or be passed as inputs to all subsequent layers when fully connected layers are employed. In order to improve the performance of deep CNNs, various architectures have been proposed. U-Net adopts symmetrical encoding and decoding paths with skip connections between them and is widely used in medical image segmentation. The residual network (ResNet) architecture employs a shortcut connection which reduces the likelihood of “vanishing” gradients during training, allowing the development of deeper networks.

### 2.2 Unsupervised learning

Supervised learning requires time-consuming and labor-intensive manual data annotations. In contrast, unsupervised techniques learn the distribution of input data and divide samples into clusters without labeled training dataset. Common unsupervised learning algorithms include the active contour model (ACM), hidden markov random fields (HMRF), the K-means and expectation-maximization (EM) algorithms, principal component analysis (PCA) and hybrid hierarchical clustering. ACM works to segment objects in an image by evolving a curve according to the constraints in the image [18]. The HMRF model is a random process generated by MRF. Its state sequence cannot be directly observed, but can be indirectly estimated through observation [165]. The EM algorithm is an iterative method that searches the (local) maximum likelihood or maximum a posteriori (MAP) estimate of the parameters in a statistical model [30]. PCA is an orthogonal linear transformation that reduces the dimensionality of

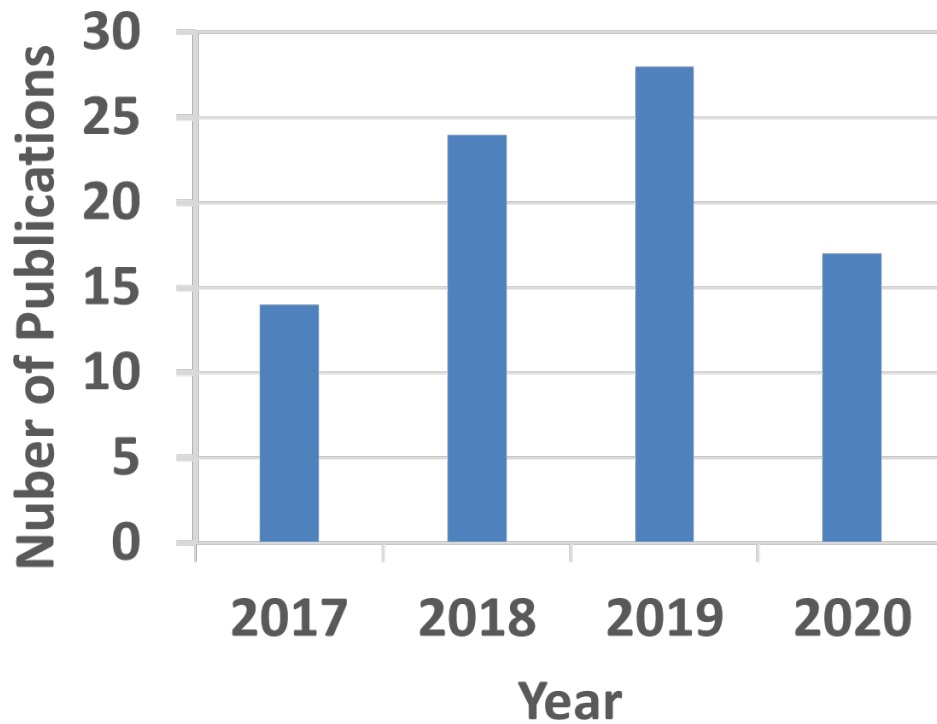


Fig. 1. Number of publications in AI-based tumor subregion analysis. “2020” only covers the first five months of 2020.

the input data while retaining its most significant parts [152]. K-means identifies  $k$  centroids and assigns each data point to the nearest centroid by minimizing the sum of the squared Euclidean distances between each point and its assigned centroid [76]. Hybrid hierarchical cluster combines the advantages of bottom-up hierarchical clustering and top-down clustering, so it is applicable to various sizes of data [24].

### 3 LITERATURE SEARCH

The scope of this review is limited to the applications of AI in tumor subregion analysis. Peer-reviewed journal publications appearing after December 31, 2016 were collected from various databases including Google Scholar, PubMed, Web of Science, etc. We used a variety of keywords such as machine learning, deep learning, intratumor, subregion, subvolume, voxel-based, overall survival, clustering. Publications describing the methods of the top three performers in the Brain tumor segmentation (BraTS) challenge from 2017-2019 were included. For all other body sites, the included publications are listed in tables accompanying each dedicated section. A total of 89 papers were identified discussing AI applications in imaging-based tumor subregion analysis. The number of publications is plotted by year in Fig 1.

## 4 AI IN TUMOR SUBREGION ANALYSIS OF MEDICAL IMAGES

### 4.1 Supervised learning in tumor subregion analysis of medical images

Supervised learning has been widely used in tumor subregion analysis for identification of recurrence volume, prediction of outcomes including overall survival (OS) or progression-free survival (PFS), and subregion segmentation. Sixty-four papers related to supervised learning are included in this paper.

TABLE I. Overview of supervised learning for tumor subregions analysis based on medical imaging for HN.

Ref	Year	Model	Task	Modality	# of patients in training/testing datasets
[32]	2017	Cox proportional hazards model	Predict OS	MRI, CT	111 (N/A)
[14]	2019	RF	Recurrence volume identification	18F-FDG PET/CT	26, LOOCV

LOOCV: leave-one-out cross-validation. N/A: not available, indicating that the paper only provides the total number of samples.

#### 4.1.1 Head and neck (HN)

CT and 18-FDG PET are often used in staging, radiation therapy treatment planning and evaluation of treatment response in patients with cancers of the head and neck [112, 124]. PET provides detailed functional and metabolic molecular information, while CT reveals the precise anatomical position of the tumor. Table 1 shows a list of selected studies that used supervised learning in tumor subregion analysis based on medical images in the head and neck. Ding et al. investigated the clinicopathological characteristics of different supraglottic subregions and their correlation with the prognosis of patients with squamous cell carcinoma [32]. Supraglottic squamous cell carcinomas were divided into four types based on subregion: epiglottis, ventricular bands, aryepiglottic fold, and ventricle. A Cox proportional hazards model was used to generate a biomarker. They found that there were significant differences in the regional control rate, overall survival rate, and cancer-specific survival rates among different subregions, indicating that patients with carcinoma of the epiglottis or ventricular bands had an increased survival rate relative to those with disease in the aryepiglottic fold or ventricle. Beaumont et al. [14] developed a voxel-wise ML model to identify the sub-regions with tumor recurrence and to predict their location based on pre-treatment PET images. A RF model was trained with voxel-wise features. Voxel-wise analysis based on radiomic features and spatial location within the tumor was shown helpful in determining the location of recurrence and providing guidance to tailor chemoradiation therapy (CRT) through dose escalation within the area of radiation resistance.

#### 4.1.2 Gliomas

Gliomas are the most common primary brain tumor and can be classified by histopathologic features into two groups: high-grade gliomas (HGG) and low-grade gliomas (LGG). Magnetic resonance imaging (MRI) is the main imaging modality to noninvasively diagnose brain tumors by providing high soft tissue contrast [13]. Dividing gliomas into substructures played an important role in glioma diagnosis, staging, monitoring and treatment planning for patients. Table 2 shows a list of selected studies using supervised learning in tumor subregion analysis based on medical images for gliomas.

Fiouznia et al. [42] developed a model to discriminate glioma tissue subregions based on multiparametric (mp) MRI. Based on the histopathological results, subregions were categorized into active tumor (AT), infiltrative edema (IE), and normal tissue (NT). In the study of Fischer et al., linear discriminant analysis (LDA), quadratic discriminant analysis (QDA), and SVM were applied to distinguish the three tissue subtypes from each other based on selected features derived from sub-regions. All three classifiers achieved the high classification performance (AUC 90%) with a combination of "CBV, MD, T<sub>2</sub>\_ISO, FLAIR" features. This capability might be advantageously employed to locate tissue subregions prior to image-guided biopsy procedures. Some studies further predicted OS or PFS based on tumor subregion analysis [87, 174].

Zhou et al. [174] developed a framework to identify tumor subregions based on pretreatment MRI for patients with glioblastoma (GBM), correlating the image-based spatial characteristics of subregions with survival rate. Two datasets were included in this study. The habitat-based features were extracted from the GBM subregions derived from intratumoral grouping and spatial mapping. The results revealed that habitat-based features were effective for predicting two survival groups (accuracy is 87.5% and 86.36%, respectively). The results generated by classifiers (SVM, k-nearest neighbors (KNN), and naïve Bayes) showed that the spatial correlation features between the signal-enhanced subregions can

effectively predict survival group ( $P < 0.05$  for all classifiers). GBM is further characterized by infiltrative growth at the cellular level that cannot be completely resected. Diffusion tensor imaging (DTI) has been shown to potentially detect tumor infiltration by reflecting microstructural destruction. To investigate the incremental prognostic value of infiltrative patterns over clinical factors and identify specific subregions that may be suitable for targeted therapy, Li et al. [87] explored the heterogeneity of GBM infiltration using joint histogram analysis in DTI. The prognostic value of covariates for OS and PFS at 12 and 18 months was tested using a logistic regression model. The results showed that joint histogram features have incremental prognostic values when combined with clinical factors, suggesting that patients may benefit from adaptive radiation therapy strategies based on prognostic data obtained during and after treatment if these high-risk tumor subregions can be identified.

CNN have achieved tremendous success in tumor subregion analysis and can be used to extract features and segment tumor subregions. Small sample size is one problem encountered with the application of CNNs to limited medical images. Transfer learning and fine-tuning may be employed to ameliorate small sample problems, making CNN more applicable to various medical image tasks [114]. Lao et al. extracted features from manually segmented tumor subregions based on multi-modality MR images and used these features to generate a proposed signature based on LASSO [84]. The extracted features included two parts: hand-crafted features and features extracted by a pre-trained deep DL model. The study demonstrated that transfer learning-based deep features were able to generate imaging signatures for OS prediction and risk stratification for GBM, indicating the potential of DL feature-based biomarkers in the preoperative care of patients with GBM. CNNs can also be used to segment tumor subregions to facilitate their further study. Based on multiparametric MRI, Kazerooni et al. [43] constructed a multi-institutional radiomics model that supports the upfront prediction of PFS and recurrence pattern (RP) in patients diagnosed with GBM at the time of initial diagnosis. The proposed framework included subregion identification (DeepMedic [75]), feature extraction, sequential forward feature selection, biomarker generation, and classification using a SVM implemented using the Cancer Imaging Phenomics Toolkit (CaPTk) open-source software. The area under the operator-received curve (AUC) for PFS prediction was 0.88 and 0.82-0.83; AUC for RP was 0.88 and 0.56-0.71 for the single-institution and multi-institutional analyses, respectively. The results suggest that the biomarkers included in the radiomics models as implemented in CaPTK could predict PFS and RP in patients diagnosed with GBM. Isocitrate dehydrogenase 1 (IDH1) is established as a prognostic and predictive marker for patients with GBM [65, 97, 108, 115, 127, 133]. Li et al. [89] developed a model to predict IDH mutation status in GBM preoperatively based on multiregional radiomic features derived from mpMRI. The proposed model was tested on an independent validation cohort. IDH1 mutation was predicted by the RF model after using Boruta [83] for feature selection. The multi-tumor subregions were automatically segmented using a CNN [117]. The model's best performance achieved 97% accuracy with AUC 0.96, and F1-score 0.84. The multi-region model built using all-region features performed better than single-region models. The multi-region model achieved the best performance when combining age with all-region features. The results showed that the proposed model based on multi-regional mpMRI features has the potential to detect IDH1 mutation status in GBM patients prior to surgery.

### 4.1.3 BraTS challenge

As mentioned above, glioma subregion segmentation may play an important role in future glioma diagnosis, staging and treatment planning. Most of the research described here uses a non-public or institutional dataset, making it difficult to compare methods or results against other published work. The BraTS challenge stands in contrast to these, providing pre-operative mpMRI scans sourced from multiple institutions to inspire and evaluate the reproducibility of state-of-the-art methods for glioma brain tumor segmentation [10, 9, 11, 12, 103]. The data set includes images of four MR sequences: T1, T1-Gd, T2, and FLAIR. The labels are divided into four classes (0: healthy tissues, 1: necrosis and non-enhancing tumor, 2: edema, 4: enhancing tumor). The evaluation system divides the tumor into three regions for performance evaluation according to practical clinical application: (1) the whole tumor (WT) region with labels 1, 2, and 4; (2) the tumor core (TC) with labels 1 and 4; (3) the enhancing tumor (ET) region (table 4).

Table 3 contains a list of selected references using supervised learning in tumor subregion analysis of BraTS challenge data. Most of these are based on DL with various proposed architectures. Attention gates are commonly adopted to improve performance due to its utility in automatically highlighting informative elements of intermediate feature maps. Hu et al. proposed a novel 3D refinement module

TABLE II. Overview of supervised learning for tumor subregions analysis based on medical imaging for gliomas.

Ref	Year	Models	Task	Modality	# of patients in training/testing datasets
[42]	2018	LDA, QDA, SVM	Predict active and infiltrative tumorous subregions	T1W, T2W, FLAIR, T2-relaxometry, DWI, DTI, IVIM, and DS-MRI	10, LOOCV
[174]	2017	SVM, KNN, Nave Bayes	Predict overall survival	T1W-ce, FLAIR, T2W	79, LOOCV
[87]	2019	logistic regression	Identify specific subregions for targeted therapy	DTI	115,(N/A*)
[84]	2017	CNN, LASSO	Predict OS	T1W, T1-Gd, FLAIR, T2W	75/37
[43]	2020	DeepMedic, SVM	Predict PFS and RP	T1W, T1-Gd, FLAIR, T2W, DWI, DS-MRI	Scheme 1 and 3:80, 10 Scheme 2: 56/24
[89]	2018	RF	Predict isocitrate dehydrogenase 1 genes (IDH1)	T1W, T1-Gd, FLAIR, T2W	118/107
[16]	2018	RF	Predict survival time	T1W-ce, FLAIR	73, LOOCV
[17]	2018	RF	Predict OS and PFS	T1W, FLAIR	40, 5 folds
[140]	2019	SVM	Glioma grading	DTI, T1W-ce, FLAIR, T2W-FSE, DSCE-RAW, 1H-MRS	40, LOOCV
[164]	2019	LASSO	stratify glioblastoma patients basd on survival	T1W, T1W-CE, FLAIR, T2W	70/35
[22]	2019	Cox proportional hazards model	stratify glioblastoma patients basd on survival	post-T1W	85/42
[132]	2018	CNN	Tumor subregions segmentation	T1W-CE	186/47

\* Exact training and testing datasets are not available.

that can aggregate local detail information and 3D semantic context directly within the 3D convolutional layer [64]. Kamnitsas et al. developed a 3D-CNN with a dual pathway and 11 convolutional layers [75]. In order to cope with the computational burden of the 3D network, the processing of adjacent image paths was combined into a channel through the network during training, while automatically adapting to the inherent class imbalances existing in the data. They used a dual-path architecture to simultaneously process multi-scale input images to obtain multi-scale context information. A 3D fully conditional random field (CRF) was employed in post-processing and was shown to be effective in mitigating false positives. Havaei et al. developed a novel CNN with a two-pathway architecture which was adopted to simultaneously extract both local and global contextual features [61]. They modeled local label dependencies by cascade-CNN rather than CRF. This method can significantly improve computational speed by employing the efficient convolution operation rather than CRFs. Due to the tremendous success of the attention mechanism in computer vision at large [51, 62, 141, 142, 150, 161] and medical image analysis specifically [1, 110, 120, 136, 162, 171], Zhang et al. integrated an attention gate into U-Net to generate an Attention Gate Residual U-Net (AGResU-Net) model for brain tumor segmentation [163]. Several attention gate units were added to the skip connection of U-Net to highlight contrast information while disambiguating irrelevant and noisy feature responses.

Table 4 lists the three top-performing studies from 2017 to 2019 with their results. Ensemble learning, cascade learning, and multi-scale operations are commonly added to CNNs to improve the accuracy of brain tumor subregion segmentation. In statistics and machine learning, ensemble learning combines models to surpass the performance of any one constituent model and is commonly used to improve classification, prediction and segmentation performance. Kamnitsas et al. [74] developed a framework (EMMA) to combine several DL models for robust segmentation. EMMA independently trained DeepMedic [75], FCN [96], and U-Net [125], combining their segmentation predictions at testing. Myronenko et al. proposed a semantic segmentation CNN with asymmetric large encoders to segment tumor subregions [106]. A variational autoencoder (VAE) branch was added to the network to reconstruct the input images jointly with the segmentation and regularize the shared encoder. Finally, they assembled ten models trained from scratch to further improve performance. Zhao et al. [169] developed a self-ensemble U-Net, combining multi-scale prediction to boost accuracy with a slight increase in memory consumption. They also used the average of all models in the final ensemble and averaged the prediction of the overlapping patches to obtain a more accurate result. Cascade learning is a particular case of ensemble learning based on the concatenation-in-series of several models, using preceding model outputs as inputs for the next model in the cascade. Wang et al. trained three networks for cascade learning, each with a similar structure, including a large encoder part with dilated convolutions and a basic decoder [144]. The WT was segmented first and bounding box of the result was used for the TC segmentation. Finally, the ET segmentation was based on the bounding box of the TC segmentation. The  $3 \times 3 \times 3$  convolution kernel was decomposed into  $3 \times 3 \times 1$  and  $1 \times 1 \times 3$  kernels to reduce the number of parameters and deal with anisotropic receptive fields. Jiang et al. [69] developed a two-stage cascaded U-Net to segment brain tumor subregions from coarse to fine-scale. In the first stage, a U-Net predicts a coarse segmentation result based on the multi-modal MRI. The coarse segmentation provides the rough locations of tumors and this is used to highlight contrast information. The coarse segmentation results are combined with the raw input images prior to input into a second U-Net with two decoder paths (one using a deconvolution, the other using trilinear interpolation) to generate a fine segmentation map. Zhou et al. [171] proposed an ensemble framework combining different networks to segment tumor subregions with more robust results. The proposed framework considered multi-scale information by segmenting three tumor subregions in cascade with a shared backbone weight and an attention block. Multi-scale and deeper networks may achieve better segmentation results because brain tumors have a highly heterogeneous appearance on MR images. Mckinly et al. [101] proposed a U-Net-like network containing a DenseNet with dilated convolutions. The author also introduced a new loss function, a generalization of binary cross-entropy, to solve label uncertainty. In another study, Mckinly et al. [102] used a structure very similar to the previous one, [101] but replaced Batch normalization with instance normalization and added a simple local attention mechanism between dilated dense blocks. This study also included more data for training so that it may also improved the performance of the network. Isensee et al. made a minor modifications to U-Net, replacing ReLU and batch normalization with leaky ReLU and instance normalization to achieve competitive performance. [68] They also supplemented with data from their own institution to achieve a 2% increase in Dice similarity coefficient (DSC) on the enhancing tumor training data.

In the past three years, BraTS has also focused on prediction of OS. Table 5 lists the top three results for

TABLE III. Overview of supervised learning in tumor subregion analysis of BraTS challenge data.

Ref	Year	Models	Task	# of patients in training/testing datasets
[61]	2017	Cascade CNN	Tumor subregion segmnetation	60, 7 fold
[75]	2017	Efficient Multi-scale U-Net with CRFs	Tumor subregion segmnetation	253, 5 fold
[64]	2020	3D refinement U-Net	Tumor subregion segmnetation	274/110
[163]	2020	Attention Gate ResU-Net	Tumor subregion segmnetation	285/46, 285/66, 335/125
[128]	2018	Emsemble CNN	Tumor subregion segmnetation	285 (N/A)
[63]	2019	multi-cascaded CNN with CRFs	Tumor subregion segmnetation	40, 274, 285
[21]	2019	3D dilated multi-fiber U-Net	Tumor subregion segmnetation	285/66
[172]	2020	Cross-task Guided Attention U-Net	Tumor subregion segmnetation	274/110, 285/46, 285/66
[105]	2019	2D-3D context U-Net	Tumor subregion segmnetation	235/50/46
[27]	2018	CNN	Tumor subregion segmnetation	240/34
[88]	2019	Inception-based U-Net	Tumor subregion segmnetation	165/55/54, 171/57/57
[168]	2018	FCNN with CRFs	Tumor subregion segmnetation	30/35, 274/110, 274/191
[25]	2018	SVM, RF, Logistic regression	Glioma grading	285, 5 fold
[122]	2020	U-Net, RF	Tumor subregion segmnetation, Predict OS	268/67, 76/29
[111]	2019	LASSO	Predict OS	163, 5 fold
[31]	2020	Heterogeneous CNN with CRFs-Recurrent Regression	Tumor subregion segmnetation	60 (N/A*)
[145]	2019	2.5D cascade CNN	Tumor subregion segmnetation	285/46/146, 285/66/191
[95]	2020	IOU 3D symmetric fully CNN	Tumor subregion segmnetation	134/33
[130]	2020	CNN	Tumor subregion segmnetation	20/10, 192/82, 285/146, 285/191
[77]	2020	CNN, SVM	Tumor subregion segmnetation	274, 10 fold
[66]	2018	CNN	Tumor subregion segmnetation	274/110
[91]	2019	CNN	Tumor subregion segmnetation	285/46, 285/66
[92]	2020	U-Net	Tumor subregion segmnetation	285/46, 285/66
[80]	2018	Hybird pyramid U-Net	Tumor subregion segmnetation	285, 5 fold
[147]	2019	CNN	Tumor subregion segmnetation	285 (N/A)
[107]	2020	CNN	Tumor subregion segmnetation	27/254,285
[134]	2020	CNN	Tumor subregion segmnetation	85/200
[123]	2020	CNN	Tumor subregion segmnetation	68/8, 50/6

\* Exact training and testing datasets are not available

TABLE IV. Overview of the top 3 segmentation performance of the last three BraTS (2017-2019).

Ref	Year	Ranking	DSC			Hausdorff95 (mm)		
			WT	TC	ET	WT	TC	ET
[74]	2017	1	0.886	0.785	0.729	5.01	23.10	36.00
[144]	2017	2	0.874	0.775	0.783	6.55	27.05	15.90
[67]	2017	3	0.858	0.775	0.647	N/A	N/A	N/A
[160]	2017	3	N/A	N/A	N/A	N/A	N/A	N/A
[106]	2018	1	0.884	0.815	0.766	3.77	4.81	3.77
[68]	2018	2	0.878	0.806	0.779	6.03	5.08	2.90
[101]	2018	3	0.886	0.799	0.732	5.52	5.53	3.48
[171]	2018	3	0.884	0.796	0.778	5.47	6.88	2.94
[69]	2019	1	0.888	0.837	0.833	4.62	4.13	2.65
[169]	2019	2	0.883	0.861	0.810	4.80	4.21	2.45
[102]	2019	3	0.890	0.830	0.810	4.85	3.99	2.74

N/A: not available, WT: Whole tumor, TC: Tumore core, and ET: Enhancing tumor.

the OS prediction task. RF regression was a popular method for this task. Shboul et al. [131] extracted 1366 textures and other features, selecting significant features in three steps. The 40 most significant features were used to train the RF regression model and predict OS. Puybureau et al. [119] extracted features from segmented tumor region and introduced patient age into the feature space. PCA was performed to normalize the training set. The feature-wise mean, standard deviation, and projection matrix ( $W$ ) were computed and stored during the rescaling phase of the PCA. The RF regression model was trained based on the normalized data. The feature vector of the test set was also normalized by the feature-wise mean and standard deviation derived from the training phase, and was then projected in the principal component space with  $W$ . The rescaled vectors were fed into the trained RF classifiers and the final prediction was obtained by majority voting. Sun et al. [135] extracted 4526 features from the tumor lesion based on their previous segmentation results. Important features were selected by decision tree and cross-validation. Finally, they trained an RF regression model to predict OS. MLP was another popular method for this task. Jungo et al. [72] computed 26 geometrical features from the segmented tumor regions and added age to complete the feature space. The four most important features were selected before being fed into a fully-connected neural network with one hidden layer and a linear activation function. Baid et al. [8] extracted features from segmented tumor regions and excluded high-correlation features by Spearman correlation. An MLP was trained with variables that demonstrated statistically significant correlation with OS. He et al. [143] selected seven features as input for a fully-connected neural network with two hidden layers. Their linear regression model also achieved good results. Feng et al. [47] extracted image features and non-imaging clinical features to construct a linear regression model. They used two-dimensional feature vectors to represent the non-image features of resection status and compensate for sparse resection status data. They used a linear regression model to fit the training data after feature normalization. Weninger et al. [151] measured the volume of subregions based on segmentation results. The volume information, the distance between the centroids of tumor and brain, and patient age were used as input for linear regression to predict OS. In addition to radiomic features, Wang et al. [149] also considered biophysical modeling of tumour growth and calculated the ratio of second semi-axis length between TC and WT, to define a novel measure termed the relative invasiveness coefficient (RIC). Following feature selection, RIC, age and radomic features were fed into the epsilon-support vector regression. The method achieved an accuracy of 0.56 in OS prediction by incorporating RIC.

## 4.2 Unsupervised learning in tumor subregion analysis of medical images

Unsupervised learning has also been widely used in tumor subregion analysis of medical images for data without available or well-defined labelled training dataset. The twenty-five papers employing unsupervised learning techniques listed in Table 6 most focus on OS and PFS prediction and identification of tumor recurrence. There are several widely-adopted unsupervised algorithms, including level set methods (LSM), thresholding, individual- and population-level clustering, and K-means.

TABLE V. Overview of the studies and results with top 3 OS prediction performance of each year from 2017 to 2019.

Ref	Year	Ranking	Accuracy	MSE	Median-SE	Std-SE
[131]	2017	1	0.579	245779.5	24944.4	726624.7
[72]	2017	2	0.568	213000.0	28100.0	662600.0
[45]	2017	3	N/A	N/A	N/A	N/A
[47]	2018	1	0.612	231746.0	34306.4	N/A
[119]	2018	2	0.605	N/A	N/A	N/A
[135]	2018	2	0.605	N/A	32895.1	N/A
[8]	2018	3	0.558	338219.4	38408.2	939986.8
[151]	2018	3	0.558	277890.0	43264	N/A
[3]	2019	1	0.579	374998.8	46483.36	1160428.9
[149]	2019	2	0.56	N/A	N/A	N/A
[46]	2019	3	0.551	N/A	N/A	N/A
[143]	2019	3	0.551	41000.0	49300.0	123000.0

N/A: not available. MSE: Mean square error

#### 4.2.1 Level Set Methods

Level set methods are commonly used for unsupervised learning applied to segmentation tasks. Cui et al. [28] developed and validated prognostic imaging biomarkers to predict OS of GBM patients based on multi-region quantitative image analysis. Each tumor was semi-automatically delineated by the level set algorithm and the segmented lesion was further divided into several subregions based on the hidden Markov random field (MRF) model and the EM algorithm [165]. The biomarker was generated based on LASSO to predict the OS of the patients with GBM, and the model was tested by an independent cohort from the local institution. The concordance index and stratification of OS using the log-rank test were 0.78 and  $P = 0.018$  for the proposed method, outperforming conventional prognostic biomarkers such as age (concordance index: 0.57,  $P = 0.389$ ) and tumor volume (concordance index: 0.59,  $P = 0.409$ ). In a later study, Cui et al. [29] defined a high-risk volume (HRV) based on mpMRI images for predicting GBM survival and investigated its relationship and synergy with molecular characteristics. Each tumor was delineated by the level set algorithm and manual correction was performed for eight failed cases. The patients with an unmethylated MGMT promoter and high HRV had significantly shorter OS (median 9.3 vs. 18.4 months, log-rank  $P = 0.002$ ), indicating the volume of the high-risk intratumoral subregion identified on mpMRI can predict survival and complement genomic information.

#### 4.2.2 Threshold-based Methods

Threshold algorithms are also suitable to separate tumor subregions based on imaging characteristics. Lawrence et al. [104] investigated whether three month treatment response of newly diagnosed GBM based on C-methionine-positron emission tomography (MET-PET) could better predict prognosis than baseline MET-PET or anatomic magnetic resonance imaging alone. A threshold of 1.5 times mean cerebellar uptake was used to automatically segment the metabolic tumor volume (MTV). Persistent MTV at three months was defined as the overlap of the three month MTV and the pre-treatment MTV. Cox proportional hazards was used to perform multivariate analysis of PFS and OS. The results showed that most patients (67%) with gross total resection (GTR) of newly diagnosed GBM have measurable post-operative MTV and that the total and persistent MTV three months post-CRT were predictors of PFS. GTV-Gd at recurrence encompassed 97% of the persistent MET-PET subvolume, 71% of the baseline MTV, 54% of the baseline GTV-Gd, and 78% of the three month MTV, respectively. The persistent MET-PET subvolume best predicts the location of tumor recurrence. Legot et al. [85] developed a framework to identify the tumor subregions of head and neck squamous cell carcinoma (HNSCC) with the risk of high recurrence on 18F-FDG PET images so that these might be considered for CRT dose escalation. Follow-up 18F-FDG PET images were registered with baseline images using an automatic rigid registration algorithm based on mutual information. Seven metabolic tumor regions were segmented in baseline images by characteristic fixed percentages of  $SUV_{max}$  and compared with two post-treatment subregions of local recurrence or residual metabolic activity. The overlap between metabolic

tumor subregions derived from baseline and follow-up PET images was only moderate.

Estrogen Receptor (ER) status is a recognized molecular feature of breast cancer correlated with prognosis and its early detection can significantly improve treatment efficacy by guiding selection of targeted therapies [4]. Chaudhury et al. developed a novel framework to classify ER status by extracting textural kinetic features from peripheral and core tumor subregions [20]. The WT was segmented using automatic threshold selection [113] combined with morphological dilation and connected component analysis. The WT was divided into two subregions according to tumor geometry. Two feature selection methods (wrapper [79] and correlation-based feature subset selection (CFS) [56]) and three classifiers (naive Bayes [70], SVM [19, 36], decision tree [121]) were adopted in this study and each feature selector followed a classifier, for a total of six model composition combinations. The best classification accuracy approached 94%, indicating that sub-region texture feature extraction can accurately classify ER status.

### 4.2.3 Individual- and population-level clustering

Individual- and population-level clustering are used to assign each pixel or voxel to suitable clusters in order to divide a tumor into subregions. After tumor subregions are obtained, the relationship between tumor subregions, OS and PFS can be investigated.

Wu et al. used individual- and population-level clustering in three works related to tumor subregion analysis. In one of their studies [154], they developed a robust tumor partitioning method to identify clinically relevant, high-risk subregions in lung cancer. The method divided the tumor into subregions based on a two stage clustering process: it first performed patient-level over-segmentation of the tumor into superpixels via K-means clustering [76] on both PET and CT images, then these superpixels were merged to subregions via population-level hierarchical clustering [71]. High-risk subregions predicted OS and out-of-field progression (OFP) over the entire cohort with a C-index of 0.66-0.67. For patients with stage III disease, the C-index reached 0.75 (HR 3.93, log-rank  $P < 0.002$ ) and 0.76 (HR 4.84, log-rank  $P < 0.002$ ) for predicting OS and OFP, respectively. In contrast, the C-index was lower than 0.60 for traditional imaging markers. The results showed that the volume of the most metabolically active and heterogeneous solid components of the tumor could predict OS and OFP better than conventional imaging markers. In a second study, Wu et al. [156] developed an imaging biomarker to assess early treatment response and predicted outcomes in oropharyngeal squamous cell carcinoma (OPSCC). Based on 18F-FDG PET and contrast CT imaging, the primary tumor and involved lymph nodes were divided into subregions by individual- and population-level clustering. The proposed imaging biomarker was generated by the LASSO algorithm. The C-index was 0.72 for the training set and 0.66 for the validation set, suggesting the proposed biomarker can accurately predict disease progression and provide patients with better risk-adapted treatment. In a third study investigating risk-stratification in breast cancer, Wu et al. divided each tumor into multiple spatially segregated, phenotypically consistent subregions based on individual- and population-level clustering, and used a net strategy to construct an imaging biomarker based on image features derived from the multiregional spatial interaction (MSI) matrix [155]. The results showed that breast cancers may exhibit three intratumoral subregions with distinct perfusion characteristics, and tumor heterogeneity may be an independent predictor of recurrence-free survival (RFS), independent of traditional predictors.

In order to predict PFS in patients with nasopharyngeal carcinoma (NPC), Xu et al. extracted subregion features via individual- and population-level clustering to generate a biomarker by LASSO [158]. Three subregions ( $S_1$ ,  $S_2$ ,  $S_3$ ) with distinct PET/CT imaging characteristics were obtained. The C-index and log-rank test for imaging biomarker  $S_3$  and WT are 0.69 and 0.58, and  $P < 0.001$  and  $P < 0.552$ , respectively, indicating  $S_3$  is superior to WT in terms of prognostic performance. Imaging biomarker  $S_3$  and American Joint Committee on Cancer (AJCC) stages III-IV were identified as independent predictors of PFS based on multivariate analysis ( $P=0.011$  and  $P=0.042$ , respectively). When combined to form a scoring system, imaging biomarker  $S_3$  and AJCC stages III-IV outperformed AJCC staging alone (log-rank test  $P < 0.0001$  vs. 0.0002;  $P < 0.0021$  vs. 0.0277 for the primary and validation cohorts, respectively). The results demonstrated that PET/CT subregion radiomics was able to predict PFS in NPC and provide prognostic information to complement other established predictors.

Even et al. [37] designed a subregional analysis for non-small cell lung cancer (NSCLC) using multi-parametric imaging. The multi-parametric images were divided into subregions in two clustering steps: each tumor was first divided into homogeneous subregions (i.e. super voxels) before being segregated

into phenotypic groups by hybrid hierarchical clustering [24]. Patients were clustered according to the absolute or relative volume of super voxels. The results showed that hypoxia, FDG avidity, and an intermediate level of blood flow/blood volume indicated a high-risk tumor type with poorer survival ( $P=0.035$ ), providing evidence of the prognostic utility of subregion classification based on multi-parametric imaging in NSCLC.

#### 4.2.4 K-means

K-means is a popular unsupervised learning method that partitions samples into  $k$  clusters. Xie et al. developed a survival prediction model for patients with oesophageal squamous cell carcinoma (OSCC) prior to concurrent CRT [157]. The patient's tumor regions were divided into subregions by K-means clustering. Radiomic features were then extracted from these sub-regions to construct a biomarker based on the LASSO algorithm and predict OS. Independent patient cohorts from another hospital were used to validate the model. The C-indices were 0.729 (0.656–0.801, 95% CI) and 0.705 (0.628–0.782, 95% CI) in the training and validation cohorts, respectively. AUC values for the 3-year survival ROC were 0.811 (0.670–0.952 95% CI) and 0.805 (0.638–0.973, 95% CI), respectively. Such a model may facilitate personalized treatment through accurate prediction of early treatment response.

Torheim et al. used K-means in MRI imaging of cervical cancer to divide voxels into two clusters based on relative signal increase (RSI) time series. Clusters of hypo-enhancing voxels demonstrated a significant correlation with locoregional recurrence ( $P=0.048$ ) [139]. Tumors with poor treatment response exhibited this characteristic in several regions, indicating a potential candidate for targeted radiotherapy.

Franklin et al. developed a method to semi-automatically segment viable and non-viable tumor regions in colorectal cancer based on DEC-MRI, and compared these with histological subregions of viable and non-viable tumor, analyzing extracted pharmacokinetic parameters between them [48]. The WT was manually delineated and four sub-regions were automatically obtained by PCA, followed by K-means. These four subregions were manually merged into two: viable and non-viable tumor. For viable tumor subregions defined by imaging and histology, DSC = 0.738 indicating the consistency of viable tumor segmentation between pre-operative DCE-MRI and postoperative histology. This technique may facilitate non-invasive assessment of treatment response in clinical practice.

#### 4.2.5 Others

Seow et al. [129] segmented the solid subregion of high-grade gliomas in MRI images by active contour modeling (ACM). The different ratio  $((s_{ACM} - s_{manual}) / s_{ACM})$ , where  $s_{ACM}$  and  $s_{manual}$  are segmented area of ACM and manual, respectively) is 1.3. This algorithm produced segmentations in under twenty minutes, while manual segmentation required an hour, demonstrating suitability for efficient segmentation of solid enhancing regions in the glioma tumor core. Fan et al. developed a framework to assess intratumoral heterogeneity in breast cancer based on the decomposition of DCE-MR images [39]. The whole breast tumor was segmented by the fuzzy C-means (FCM) algorithm [159]. A convex analysis of mixtures (CAM) method was then used to differentiate heterogeneous regions. Imaging features extracted from these regions were used predict prognosis and identify gene signatures. The results showed that tumor heterogeneity was negatively correlated with survival and the presence of cancer-related genetic markers of breast cancer. Wang et al. studied primary and secondary intrahepatic malignancies to determine whether an increase in tumor subvolume with elevated arterial perfusion during RT can predict tumor progression following treatment [146]. The arterial perfusion of tumors prior to treatment were clustered into low-normal and elevated perfusion by global-initiated regularized local fuzzy clustering (GIRLFC) [148]. The tumor sub-volumes with elevated arterial perfusion were extracted from the hepatic arterial perfusion images. The changes in tumor sub-volumes and arterial perfusion averaged over the tumors from pre-treatment baseline to mid-treatment were investigated for prediction of tumor progression following treatment. The results showed that an increase in intrahepatic subvolume with elevated arterial perfusion during RT may be a predictor of post-treatment tumor progression (AUC = 0.9). Lucia et al. [99] developed a framework to evaluate the overlap between the initial high-uptake sub-volume ( $V_1$ ) on baseline 18F-FDG PET/CT images and the metabolic relapse ( $V_2$ ) after chemoradiotherapy in locally advanced cervical cancer. CT images of recurrence were registered with baseline CT using the 3D Slicer Expert Automated Registration module [44] to obtain the

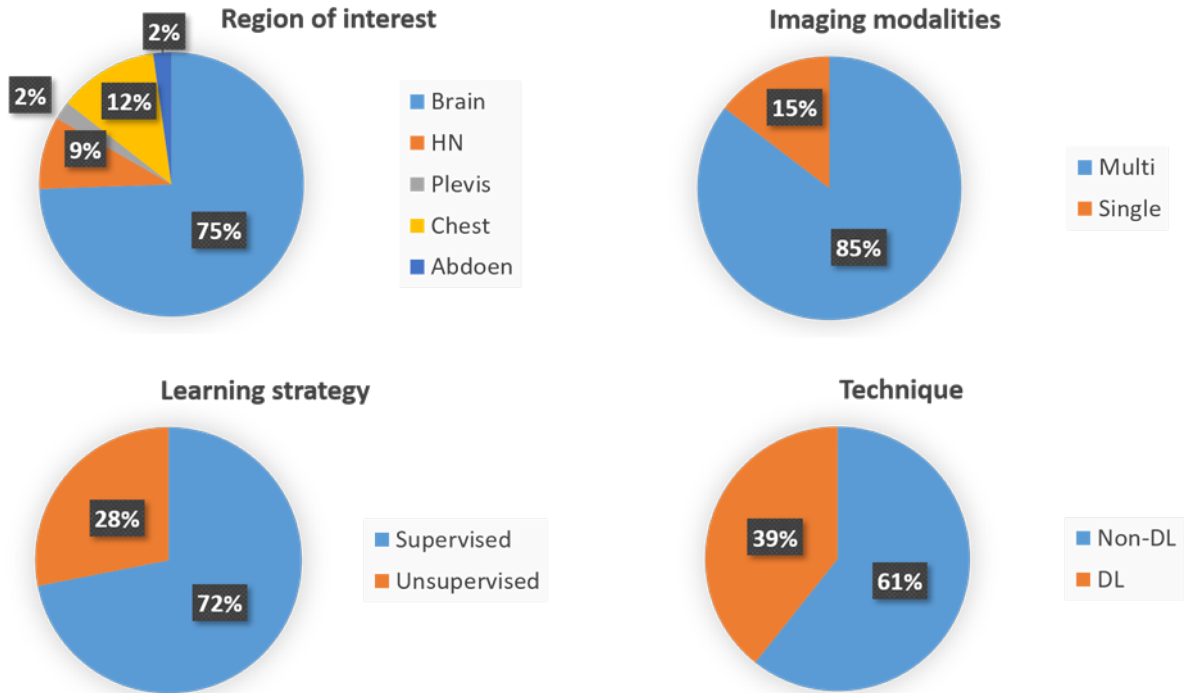


Figure 2. Pie charts for the distribution of various methods in AI-based tumor subregion analysis in medical imaging. HN: head and neck, DL: deep learning.

deformation fields by optimizing the Mattes mutual information metric [100], and the corresponding PET images were registered using the corresponding deformation fields. The fuzzy locally adaptive Bayesian (FLAB) algorithm [58] was used to determine the sub-volumes  $V_1$  and  $V_2$  for baseline and follow-up PET images. The overlaps between the baseline high-uptake sub-volume and the recurrent metabolic volume were moderate to good (range (mean  $\pm$  std)): 0.62–0.81 ( $0.72 \pm 0.05$ ), 0.72–1.00 ( $0.85 \pm 0.10$ ), 0.55–1.00 ( $0.73 \pm 0.16$ ) and 0.50–1.00 ( $0.76 \pm 0.12$ ) for DSC, overlap fraction, X ( $X = \frac{V_1 \cap V_2}{V_1}$ ) and Y ( $Y = \frac{V_1 \cap V_2}{V_2}$ ), respectively.

## 5 PREVALENCE OF METHODS

We have analyzed the percentage distribution of some attributes including the region of interest (ROI), learning strategy (supervised/unsupervised), technique (deep learning/non-deep learning), and imaging modalities (single/multi) (Figure 2). Brain and chest sites are the most studied regions of interest, with brain being most studied overall, likely in part due to the BraTS challenge providing public data as well as ground-truth for the non-public data. Supervised learning accounts for 72% of works reviewed, owing to the greater reliability and transparency of training when ground truth is available. The category of multi-modal studies account for 85% of all works while the single-modality accounts for 15%. A Non deep-learning strategy is employed in 61% of the summarized studies.

## 6 SUMMARY AND OUTLOOK

AI methods from the field of computer vision have been widely adopted to complete several tasks in tumor subregion analysis. As reviewed in here, brain is the most commonly studied site followed by chest. Since the subregions of brain tumors are generally accompanied by ground-truth data, supervised learning methods are more commonly employed than unsupervised strategies. For other body sites, unsupervised methods are more popular due to the lack of ground-truth.

Currently, there is no universal image acquisition protocol for any imaging modality in clinical practice for sub-region analysis. Images acquired from different sites and scanners may affect the performance

TABLE VI. Unsupervised learning for tumor subregions analysis. HN: head and neck.

Ref	Year	Models	Modality	Task
[28]	2016	Level set, MRF, EM	Post-T1W, FLAIR	Predict OS
[29]	2017	level set	T1W-ce, DWI	Predict OS
[104]	2019	Threshold, Cox proportional hazards	(11)C-MET-PET, T1W-Gd, FLAIR	Recurrence tumor identification predict PFS
[85]	2018	Threshold	18F-FDG PET/CT	Recurrence volume identification
[20]	2014	Threshold, SVM, Nave Bayes, decision tree, wrapper, CFS	DCE-MRI	Estrogen receptor (ER) classification
[154]	2016	Individual- and population-level clustering	18F-FDG /CT	Predict OS and OFD
[156]	2020	Individual- and population-level clustering	18F-FDG PET/CT	Assess early response and predict PFS
[155]	2018	Individual- and population-level clustering	DCE-MRI	Predict RFS
[158]	2019	Individual- and population-level clustering LASSO	18F-FDG PET/CT	Predict PFS
[37]	2017	Individual- and population-level clustering	PDG PET, CT, DCE-MRI, HX4 PET	Predict OS
[157]	2019	K-means, LASSO	CT	Predict OS
[139]	2016	k-means	DCE-MRI	Recurrence tumor identification
[48]	2020	K-means, PCA	DCE-MRI	Tumor subregion segmentation
[129]	2016	ACM	Post-T1W, FLAIR, T2W	Tumor subregion segmentation
[38]	2018	K-means	DCE-MRI	Predict prognosis
[39]	2019	FCM, CAM	DCE-MRI	Predict OS and RFS
[146]	2014	GIRLFC	DCE-MRI	Predict tumor progression after RT
[60]	2019	FLAB	18F-FDG PET/CT	Tumor subregion segmentation
[148]	2012	GIRLFC	DCE-MRI	Predict subvolume related treatment outcome
[7]	2019	3D Level set	18F-FDG PET/CT	Predict OS
[81]	2018	PCA	DCE-MRI, DWI, PET/CT	Predict neoadjuvant therapy response
[40]	2019	CAM, RF	DCE-MRI	Predict breast cancer subtypes
[98]	2020	TTP, SVM, LASSO	DCE-MRI	Predict HER2 2+ status in breast cancer
[99]	2020	FLAB	18F-FDG PET/CT	Recurrence tumor identification
[78]	2019	K-means	DWI, PET	Segmentation and Predict

of these models. In order to address this issue, the quantitative imaging biomarkers alliance (QIBA) [15] and the quantitative imaging network (QIN) [73] have been working to formalize a standard imaging protocol.

Sample sizes in the reviewed studies were small to intermediate (median (range): 230 (4-626)). For supervised learning, a large training set is required to train a reliable model. A large validation set is also essential in rigorously evaluating the proposed methods. Except for the BraTS studies, most reviewed here used institutional data and may lack generalizability. Many studies on tumor sub-regions demonstrate correlations to survival, as well as treatment response and recurrence. To validate these findings, significant time must be invested in follow-up especially in diseases with low overall mortality. Validation may also be confounded by adjuvant treatment during the follow-up period, complicating the analysis of any relationships that are discovered.

Deep learning has demonstrated clinical utility in many tasks in medical imaging. At the time of writing, tumor subregion analysis is primarily in use for brain tumor subregion segmentation, but is rarely used in non-segmentation tasks or in other body sites. Great potential remains for DL applications in tumor subregion analysis. First, a CNN might be used to automatically extract useful features rather than relying upon handcrafted features. Secondly, for clinical tasks for which it is difficult to obtain manually-annotated ground truth data, an unsupervised CNN has been applied to solve the segmentation problem. As an example, Zhou et al. proposed a deep image clustering model to assign pixels to different clusters by updating cluster associations and cluster centers iteratively [173]. Thirdly, CNN could be used to generate radiomic signatures for various clinical applications based on tumor subregion such as OS prediction, treatment response prediction and clinical risk stratification. In order to realize the full potential of DL applications in tumor subregion analysis, models must be trained on large datasets with external cross-site validation.

## 7 Summary and Discussion

GANs have been increasingly used in the application of medical/biomedical imaging. As reviewed in this chapter, cGAN- and Cycle-GAN-based image synthesis is an emerging active research field with all these reviewed studies published within the last few years. With the development in both artificial intelligence and computing hardware, more GAN-based methods are expected to facilitate the clinical workflow with novel applications. Compared with conventional model-based methods, GAN-based methods are more generalized since the same network and architecture for a pair of image modalities can be applied to different pairs of image modalities with minimal adjustment. This allows easy extension of the applications using a similar methodology to a variety of imaging modalities for image synthesis. GAN-based methods generally outperform conventional methods in generating more realistic synthetic images with higher similarity to real images and better quantitative metrics. In implementation, depending on the hardware, training a GAN-based model usually takes several hours to days. However, once the model is trained, it can be applied to new patients to generate synthetic images within a few seconds or minutes. Due to these advantages, GAN-based methods have attracted great research and clinical interest in medical imaging and biomedical imaging.

Although the reviewed literatures show the success of GAN-based image synthesis in various applications, there are still some open questions that need to be answered in future studies. Firstly, for the training of GAN-based model, most of the reviewed studies require paired datasets, i.e., the source image and target image need to have pixel-to-pixel correspondence. This requirement poses difficulties in collecting sufficient eligible datasets, as well as demands high accuracy in image registration. As compared to cGAN, it is demonstrated that Cycle-GAN can relax the requirement of the paired datasets to be unpaired datasets, which can be beneficial for clinical application in enrolling large number of patient datasets for training. However, even the image quality derived by Cycle-GAN can be better than cGAN, the numerical performance may not be improved significantly in some synthesis tasks due to the residual mismatch between synthetic image and ground truth target image.

Secondly, although the merits of GAN-based methods have been demonstrated, its performance can be inconsistent under the circumstances that the input images are drastically different from its training datasets. As a matter of fact, unusual cases are generally excluded in most of the reviewed studies. Therefore, these unusual cases, which do happen occasionally in clinic setting, should be dealt with caution when using GAN-based methods to generate synthetic image. For example, some patients have

hip prosthesis. The hip prosthesis creates severe artifacts on both CT and MR images. The related effect of its inclusion in training or testing dataset towards network performance is an important question that has not been studied yet. There are more unusual cases that could exist in all those imaging modalities and are worth of investigation, just to name a few: all kinds of implants that introduce artifacts, obese patients whose scan has higher noise level on image than average, and patients with anatomical abnormality. To conclude, the research in image synthesis is still wide open. The authors are expected to see more activities in this domain for the years to come.

## ACKNOWLEDGEMENTS

This research was supported in part by the National Cancer Institute of the National Institutes of Health under Award Number R01CA215718 and Emory Winship Cancer Institute pilot grant.

## CONFLICT OF INTEREST

The authors declare no conflicts of interest.

## References

- [1] Nabila Abraham and Naimul Mefraz Khan. A novel focal tversky loss function with improved attention u-net for lesion segmentation. In *2019 IEEE 16th International Symposium on Biomedical Imaging (ISBI 2019)*, pages 683–687. IEEE. ISBN 1538636417.
- [2] Hugo JWL Aerts, Emmanuel Rios Velazquez, Ralph TH Leijenaar, Chintan Parmar, Patrick Grossmann, Sara Carvalho, Johan Bussink, René Monshouwer, Benjamin Haibe-Kains, and Derek Ritveld. Decoding tumour phenotype by noninvasive imaging using a quantitative radiomics approach. *Nature communications*, 5(1):1–9, 2014. ISSN 2041-1723.
- [3] Rupal R Agravat and Mehul S Raval. Brain tumor segmentation and survival prediction. In *International MICCAI Brainlesion Workshop*, pages 338–348. Springer.
- [4] Arfan Ahmed, Peter Gibbs, Martin Pickles, and Lindsay Turnbull. Texture analysis in assessment and prediction of chemotherapy response in breast cancer. *Journal of Magnetic Resonance Imaging*, 38(1):89–101, 2013. ISSN 1053-1807.
- [5] Marios Anthimopoulos, Stergios Christodoulidis, Lukas Ebner, Andreas Christe, and Stavroula Mougialakou. Lung pattern classification for interstitial lung diseases using a deep convolutional neural network. *IEEE transactions on medical imaging*, 35(5):1207–1216, 2016. ISSN 0278-0062.
- [6] Otso Arponen, Mazen Sudah, Amro Masarwah, Mikko Taina, Suvi Rautiainen, Mervi Könönen, Reijo Sironen, Veli-Matti Kosma, Anna Sutela, and Juhana Hakumäki. Diffusion-weighted imaging in 3.0 tesla breast mri: diagnostic performance and tumor characterization using small sub-regions vs. whole tumor regions of interest. *PLoS One*, 10(10):e0138702, 2015. ISSN 1932-6203.
- [7] Mehdi Astaraki, Chunliang Wang, Giulia Buizza, Iuliana Toma-Dasu, Marta Lazzeroni, and Örjan Smedby. Early survival prediction in non-small cell lung cancer from pet/ct images using an intra-tumor partitioning method. *Physica Medica*, 60:58–65, 2019. ISSN 1120-1797.
- [8] Ujjwal Baid, Sanjay Talbar, Swapnil Rane, Sudeep Gupta, Meenakshi H Thakur, Aliasgar Moiyadi, Siddhesh Thakur, and Abhishek Mahajan. Deep learning radiomics algorithm for gliomas (drag) model: a novel approach using 3d unet based deep convolutional neural network for predicting survival in gliomas. In *International MICCAI Brainlesion Workshop*, pages 369–379. Springer.
- [9] Spyridon Bakas, Hamed Akbari, Aristeidis Sotiras, Michel Bilello, Martin Rozycki, Justin Kirby, John Freymann, Keyvan Farahani, and Christos Davatzikos. Segmentation labels and radiomic features for the pre-operative scans of the tcga-igg collection. *The cancer imaging archive*, 286, 2017.

- [10] Spyridon Bakas, Hamed Akbari, Aristeidis Sotiras, Michel Bilello, Martin Rozycki, Justin Kirby, John Freymann, Keyvan Farahani, and Christos Davatzikos. Segmentation labels and radiomic features for the pre-operative scans of the tcga-gbm collection. the cancer imaging archive. *Nat Sci Data*, 4:170117, 2017.
- [11] Spyridon Bakas, Hamed Akbari, Aristeidis Sotiras, Michel Bilello, Martin Rozycki, Justin S Kirby, John B Freymann, Keyvan Farahani, and Christos Davatzikos. Advancing the cancer genome atlas glioma mri collections with expert segmentation labels and radiomic features. *Scientific data*, 4: 170117, 2017. ISSN 2052-4463.
- [12] Spyridon Bakas, Mauricio Reyes, Andras Jakab, Stefan Bauer, Markus Rempfler, Alessandro Crimi, Russell Takeshi Shinohara, Christoph Berger, Sung Min Ha, and Martin Rozycki. Identifying the best machine learning algorithms for brain tumor segmentation, progression assessment, and overall survival prediction in the brats challenge. *arXiv preprint arXiv:1811.02629*, 2018.
- [13] Stefan Bauer, Roland Wiest, Lutz-P Nolte, and Mauricio Reyes. A survey of mri-based medical image analysis for brain tumor studies. *Physics in Medicine and Biology*, 58(13):R97, 2013. ISSN 0031-9155.
- [14] J Beaumont, Oscar Acosta, A Devillers, X Palard-Novello, E Chajon, R de Crevoisier, and J Castelli. Voxel-based identification of local recurrence sub-regions from pre-treatment pet/ct for locally advanced head and neck cancers. *EJNMMI research*, 9(1):90, 2019. ISSN 2191-219X.
- [15] Andrew J Buckler, Linda Bresolin, N Reed Dunnick, Daniel C Sullivan, and Group. A collaborative enterprise for multi-stakeholder participation in the advancement of quantitative imaging. *Radiology*, 258(3):906–914, 2011. ISSN 0033-8419.
- [16] Ahmad Chaddad, Paul Daniel, Christian Desrosiers, Matthew Toews, and Bassam Abdulkarim. Novel radiomic features based on joint intensity matrices for predicting glioblastoma patient survival time. *IEEE journal of biomedical and health informatics*, 23(2):795–804, 2018. ISSN 2168-2194.
- [17] Ahmad Chaddad, Siham Sabri, Tamim Niazi, and Bassam Abdulkarim. Prediction of survival with multi-scale radiomic analysis in glioblastoma patients. *Medical and biological engineering and computing*, 56(12):2287–2300, 2018. ISSN 0140-0118.
- [18] Tony F Chan and Luminita A Vese. Active contours without edges. *IEEE Transactions on image processing*, 10(2):266–277, 2001. ISSN 1057-7149.
- [19] Chih-Chung Chang and Chih-Jen Lin. Libsvm: A library for support vector machines. *ACM transactions on intelligent systems and technology (TIST)*, 2(3):1–27, 2011. ISSN 2157-6904.
- [20] Baishali Chaudhury, Mu Zhou, Dmitry B Goldgof, Lawrence O Hall, Robert A Gatenby, Robert J Gillies, and Jennifer S Drukteinis. Using features from tumor subregions of breast dce-mri for estrogen receptor status prediction. In *2014 IEEE International Conference on Systems, Man, and Cybernetics (SMC)*, pages 2624–2629. IEEE. ISBN 1479938408.
- [21] Chen Chen, Xiaopeng Liu, Meng Ding, Junfeng Zheng, and Jiangyun Li. 3d dilated multi-fiber network for real-time brain tumor segmentation in mri. In *International Conference on Medical Image Computing and Computer-Assisted Intervention*, pages 184–192. Springer.
- [22] Xin Chen, Mengjie Fang, Di Dong, Lingling Liu, Xiangdong Xu, Xinhua Wei, Xinqing Jiang, Lei Qin, and Zaiyi Liu. Development and validation of a mri-based radiomics prognostic classifier in patients with primary glioblastoma multiforme. *Academic radiology*, 26(10):1292–1300, 2019. ISSN 1076-6332.
- [23] Xueli Chen, Mingquan Lin, He Cui, Yimin Chen, Arna van Engelen, Marleen de Bruijne, M Reza Azarpazhooh, Seyed Mojtaba Sohrevardi, Tommy WS Chow, and J David Spence. Three-dimensional ultrasound evaluation of the effects of pomegranate therapy on carotid plaque texture using locality preserving projection. *Computer Methods and Programs in Biomedicine*, 184: 105276, 2020. ISSN 0169-2607.
- [24] Hugh Chipman and Robert Tibshirani. Hybrid hierarchical clustering with applications to microarray data. *Biostatistics*, 7(2):286–301, 2006. ISSN 1468-4357.

- [25] Hwan-ho Cho, Seung-hak Lee, Jonghoon Kim, and Hyunjin Park. Classification of the glioma grading using radiomics analysis. *PeerJ*, 6:e5982, 2018. ISSN 2167-8359.
- [26] Thibaud P Coroller, Patrick Grossmann, Ying Hou, Emmanuel Rios Velazquez, Ralph TH Leijenaar, Gretchen Hermann, Philippe Lambin, Benjamin Haibe-Kains, Raymond H Mak, and Hugo JW Aerts. Ct-based radiomic signature predicts distant metastasis in lung adenocarcinoma. *Radiotherapy and Oncology*, 114(3):345–350, 2015. ISSN 0167-8140.
- [27] Shaoguo Cui, Lei Mao, Jingfeng Jiang, Chang Liu, and Shuyu Xiong. Automatic semantic segmentation of brain gliomas from mri images using a deep cascaded neural network. *Journal of healthcare engineering*, 2018, 2018. ISSN 2040-2295.
- [28] Yi Cui, Khin Khin Tha, Shunsuke Terasaka, Shigeru Yamaguchi, Jeff Wang, Kohsuke Kudo, Lei Xing, Hiroki Shirato, and Ruijiang Li. Prognostic imaging biomarkers in glioblastoma: development and independent validation on the basis of multiregion and quantitative analysis of mr images. *Radiology*, 278(2):546–553, 2016. ISSN 0033-8419.
- [29] Yi Cui, Shangjie Ren, Khin Khin Tha, Jia Wu, Hiroki Shirato, and Ruijiang Li. Volume of high-risk intratumoral subregions at multi-parametric mr imaging predicts overall survival and complements molecular analysis of glioblastoma. *European Radiology*, 27(9):3583–3592, 2017. ISSN 0938-7994.
- [30] Arthur P Dempster, Nan M Laird, and Donald B Rubin. Maximum likelihood from incomplete data via the em algorithm. *Journal of the Royal Statistical Society: Series B (Methodological)*, 39(1):1–22, 1977. ISSN 0035-9246.
- [31] Wu Deng, Qinke Shi, Miye Wang, Bing Zheng, and Ning Ning. Deep learning-based hcn and crf-rrnn model for brain tumor segmentation. *IEEE Access*, 8:26665–26675, 2020. ISSN 2169-3536.
- [32] Weiquan Ding, Tianrun Liu, Jiangang Liang, Tingbao Hu, Shaoyun Cui, Guorong Zou, Weiwei Cai, and Ankui Yang. Supraglottic squamous cell carcinomas have distinctive clinical features and prognosis based on subregion. *Plos one*, 12(11):e0188322, 2017. ISSN 1932-6203.
- [33] Xue Dong, Yang Lei, Tonghe Wang, Matthew Thomas, Leonardo Tang, Walter J Curran, Tian Liu, and Xiaofeng Yang. Automatic multiorgan segmentation in thorax ct images using u-net-gan. *Medical physics*, 46(5):2157–2168, 2019. ISSN 0094-2405.
- [34] Xue Dong, Tonghe Wang, Yang Lei, Kristin Higgins, Tian Liu, Walter J Curran, Hui Mao, Jonathon A Nye, and Xiaofeng Yang. Synthetic ct generation from non-attenuation corrected pet images for whole-body pet imaging. *Physics in Medicine and Biology*, 64(21):215016, 2019. ISSN 0031-9155.
- [35] Xue Dong, Yang Lei, Tonghe Wang, Kristin Higgins, Tian Liu, Walter J Curran, Hui Mao, Jonathon A Nye, and Xiaofeng Yang. Deep learning-based attenuation correction in the absence of structural information for whole-body positron emission tomography imaging. *Physics in Medicine and Biology*, 65(5):055011, 2020. ISSN 0031-9155.
- [36] Yasser El-Manzalawy and Vasant Honavar. Wlsvm: integrating libsvm into weka environment. *Software available at <http://www.cs.iastate.edu/yasser/wlsvm>*, 2005.
- [37] Aniek JG Even, Bart Reymen, Matthew D La Fontaine, Marco Das, Felix M Mottaghy, José SA Belderbos, Dirk De Ruysscher, Philippe Lambin, and Wouter van Elmp. Clustering of multi-parametric functional imaging to identify high-risk subvolumes in non-small cell lung cancer. *Radiotherapy and Oncology*, 125(3):379–384, 2017. ISSN 0167-8140.
- [38] Ming Fan, Hu Cheng, Peng Zhang, Xin Gao, Juan Zhang, Guoliang Shao, and Lihua Li. Dcmri texture analysis with tumor subregion partitioning for predicting ki-67 status of estrogen receptor-positive breast cancers. *Journal of Magnetic Resonance Imaging*, 48(1):237–247, 2018. ISSN 1053-1807.

- [39] Ming Fan, Pingping Xia, Bin Liu, Lin Zhang, Yue Wang, Xin Gao, and Lihua Li. Tumour heterogeneity revealed by unsupervised decomposition of dynamic contrast-enhanced magnetic resonance imaging is associated with underlying gene expression patterns and poor survival in breast cancer patients. *Breast Cancer Research*, 21(1):112, 2019. ISSN 1465-542X.
- [40] Ming Fan, Peng Zhang, Yue Wang, Weijun Peng, Shiwei Wang, Xin Gao, Maosheng Xu, and Lihua Li. Radiomic analysis of imaging heterogeneity in tumours and the surrounding parenchyma based on unsupervised decomposition of dce-mri for predicting molecular subtypes of breast cancer. *European radiology*, 29(8):4456–4467, 2019. ISSN 0938-7994.
- [41] Reza Farjam, Christina I Tsien, Felix Y Feng, Diana Gomez-Hassan, James A Hayman, Theodore S Lawrence, and Yue Cao. Physiological imaging-defined, response-driven subvolumes of a tumor. *International Journal of Radiation Oncology\* Biology\* Physics*, 85(5):1383–1390, 2013. ISSN 0360-3016.
- [42] Anahita Fathi Kazerooni, Mahnaz Nabil, Mehdi Zeinali Zadeh, Kavous Firouznia, Farid Azmoudeh-Ardalan, Alejandro F Frangi, Christos Davatzikos, and Hamidreza Saligheh Rad. Characterization of active and infiltrative tumorous subregions from normal tissue in brain gliomas using multiparametric mri. *Journal of Magnetic Resonance Imaging*, 48(4):938–950, 2018. ISSN 1053-1807.
- [43] Anahita Fathi Kazerooni, Hamed Akbari, Gaurav Shukla, Chaitra Badve, Jeffrey D Rudie, Chiharu Sako, Saima Rathore, Spyridon Bakas, Sarthak Pati, and Ashish Singh. Cancer imaging phenomics via captk: Multi-institutional prediction of progression-free survival and pattern of recurrence in glioblastoma. *JCO Clinical Cancer Informatics*, 4:234–244, 2020. ISSN 2473-4276.
- [44] Andriy Fedorov, Reinhard Beichel, Jayashree Kalpathy-Cramer, Julien Finet, Jean-Christophe Fillion-Robin, Sonia Pujol, Christian Bauer, Dominique Jennings, Fiona Fennessy, and Milan Sonka. 3d slicer as an image computing platform for the quantitative imaging network. *Magnetic resonance imaging*, 30(9):1323–1341, 2012. ISSN 0730-725X.
- [45] Xue Feng and Craig Meyer. Patch-based 3d u-net for brain tumor segmentation. In *International Conference on Medical Image Computing and Computer-Assisted Intervention (MICCAI)*.
- [46] Xue Feng, Quan Dou, Nicholas Tustison, and Craig Meyer. Brain tumor segmentation with uncertainty estimation and overall survival prediction. In *International MICCAI Brainlesion Workshop*, pages 304–314. Springer.
- [47] Xue Feng, Nicholas J Tustison, Sohil H Patel, and Craig H Meyer. Brain tumor segmentation using an ensemble of 3d u-nets and overall survival prediction using radiomic features. *Frontiers in Computational Neuroscience*, 14:25, 2020. ISSN 1662-5188.
- [48] James M Franklin, Benjamin Irving, Bartłomiej W Papież, Jesper F Kallehauge, Lai Mun Wang, Robert D Goldin, Adrian L Harris, Ewan M Anderson, Julia A Schnabel, and Michael A Chappell. Tumour subregion analysis of colorectal liver metastases using semi-automated clustering based on dce-mri: Comparison with histological subregions and impact on pharmacokinetic parameter analysis. *European Journal of Radiology*, page 108934, 2020. ISSN 0720-048X.
- [49] David V Fried, Susan L Tucker, Shouhao Zhou, Zhongxing Liao, Osama Mawlawi, Geoffrey Ibbott, and Laurence E Court. Prognostic value and reproducibility of pretreatment ct texture features in stage iii non-small cell lung cancer. *International Journal of Radiation Oncology\* Biology\* Physics*, 90(4):834–842, 2014. ISSN 0360-3016.
- [50] Huazhu Fu, Jun Cheng, Yanwu Xu, Damon Wing Kee Wong, Jiang Liu, and Xiaochun Cao. Joint optic disc and cup segmentation based on multi-label deep network and polar transformation. *IEEE transactions on medical imaging*, 37(7):1597–1605, 2018. ISSN 0278-0062.
- [51] Jun Fu, Jing Liu, Haijie Tian, Yong Li, Yongjun Bao, Zhiwei Fang, and Hanqing Lu. Dual attention network for scene segmentation. In *Proceedings of the IEEE Conference on Computer Vision and Pattern Recognition*, pages 3146–3154.

- [52] Yabo Fu, Thomas R Mazur, Xue Wu, Shi Liu, Xiao Chang, Yonggang Lu, H Harold Li, Hyun Kim, Michael C Roach, and Lauren Henke. A novel mri segmentation method using cnn-based correction network for mri-guided adaptive radiotherapy. *Medical physics*, 45(11):5129–5137, 2018. ISSN 0094-2405.
- [53] Robert A Gatenby, Olya Grove, and Robert J Gillies. Quantitative imaging in cancer evolution and ecology. *Radiology*, 269(1):8–14, 2013. ISSN 0033-8419.
- [54] Olya Grove, Anders E Berglund, Matthew B Schabath, Hugo JWL Aerts, Andre Dekker, Hua Wang, Emmanuel Rios Velazquez, Philippe Lambin, Yuhua Gu, and Yoganand Balagurunathan. Quantitative computed tomographic descriptors associate tumor shape complexity and intratumor heterogeneity with prognosis in lung adenocarcinoma. *PLoS one*, 10(3):e0118261, 2015. ISSN 1932-6203.
- [55] Zaiwang Gu, Jun Cheng, Huazhu Fu, Kang Zhou, Huaying Hao, Yitian Zhao, Tianyang Zhang, Shenghua Gao, and Jiang Liu. Ce-net: Context encoder network for 2d medical image segmentation. *IEEE transactions on medical imaging*, 38(10):2281–2292, 2019. ISSN 0278-0062.
- [56] Mark A Hall. Correlation-based feature subset selection for machine learning. *Thesis submitted in partial fulfillment of the requirements of the degree of Doctor of Philosophy at the University of Waikato*, 1998.
- [57] Joseph Harms, Yang Lei, Tonghe Wang, Rongxiao Zhang, Jun Zhou, Xiangyang Tang, Walter J Curran, Tian Liu, and Xiaofeng Yang. Paired cycle-gan-based image correction for quantitative cone-beam computed tomography. *Medical physics*, 46(9):3998–4009, 2019. ISSN 0094-2405.
- [58] Mathieu Hatt, Catherine Cheze Le Rest, Alexandre Turzo, Christian Roux, and Dimitris Visvikis. A fuzzy locally adaptive bayesian segmentation approach for volume determination in pet. *IEEE transactions on medical imaging*, 28(6):881–893, 2009. ISSN 0278-0062.
- [59] Mathieu Hatt, Mohamed Majdoub, Martin Vallières, Florent Tixier, Catherine Cheze Le Rest, David Groheux, Elif Hindié, Antoine Martineau, Olivier Pradier, and Roland Hustinx. 18f-fdg pet uptake characterization through texture analysis: investigating the complementary nature of heterogeneity and functional tumor volume in a multi-cancer site patient cohort. *Journal of nuclear medicine*, 56(1):38–44, 2015. ISSN 0161-5505.
- [60] Mathieu Hatt, Florent Tixier, Marie-Charlotte Desseroit, Bogdan Badic, Baptiste Laurent, Dimitris Visvikis, and Catherine Cheze Le Rest. Revisiting the identification of tumor sub-volumes predictive of residual uptake after (chemo) radiotherapy: influence of segmentation methods on 18f-fdg pet/ct images. *Scientific reports*, 9, 2019.
- [61] Mohammad Havaei, Axel Davy, David Warde-Farley, Antoine Biard, Aaron Courville, Yoshua Bengio, Chris Pal, Pierre-Marc Jodoin, and Hugo Larochelle. Brain tumor segmentation with deep neural networks. *Medical image analysis*, 35:18–31, 2017. ISSN 1361-8415.
- [62] Jie Hu, Li Shen, and Gang Sun. Squeeze-and-excitation networks. In *Proceedings of the IEEE conference on computer vision and pattern recognition*, pages 7132–7141.
- [63] Kai Hu, Qinghai Gan, Yuan Zhang, Shuhua Deng, Fen Xiao, Wei Huang, Chunhong Cao, and Xieping Gao. Brain tumor segmentation using multi-cascaded convolutional neural networks and conditional random field. *IEEE Access*, 7:92615–92629, 2019. ISSN 2169-3536.
- [64] Xiaojun Hu, Weijian Luo, Jiliang Hu, Sheng Guo, Weilin Huang, Matthew R Scott, Roland Wiest, Michael Dahlweid, and Mauricio Reyes. Brain segnet: 3d local refinement network for brain lesion segmentation. *BMC medical imaging*, 20(1):17, 2020. ISSN 1471-2342.
- [65] Koichi Ichimura, Danita M Pearson, Sylvia Kocialkowski, L Magnus Backlund, Raymond Chan, David TW Jones, and V Peter Collins. Idh1 mutations are present in the majority of common adult gliomas but rare in primary glioblastomas. *Neuro-oncology*, 11(4):341–347, 2009. ISSN 1522-8517.
- [66] Sajid Iqbal, M Usman Ghani, Tanzila Saba, and Amjad Rehman. Brain tumor segmentation in multi-spectral mri using convolutional neural networks (cnn). *Microscopy research and technique*, 81(4):419–427, 2018. ISSN 1059-910X.

- [67] Fabian Isensee, Philipp Kickingereder, Wolfgang Wick, Martin Bendszus, and Klaus H Maier-Hein. Brain tumor segmentation and radiomics survival prediction: Contribution to the brats 2017 challenge. In *International MICCAI Brainlesion Workshop*, pages 287–297. Springer, .
- [68] Fabian Isensee, Philipp Kickingereder, Wolfgang Wick, Martin Bendszus, and Klaus H Maier-Hein. No new-net. In *International MICCAI Brainlesion Workshop*, pages 234–244. Springer, .
- [69] Zeyu Jiang, Changxing Ding, Minfeng Liu, and Dacheng Tao. Two-stage cascaded u-net: 1st place solution to brats challenge 2019 segmentation task. In *International MICCAI Brainlesion Workshop*, pages 231–241. Springer.
- [70] George H John and Pat Langley. Estimating continuous distributions in bayesian classifiers. *arXiv preprint arXiv:1302.4964*, 2013.
- [71] Stephen C Johnson. Hierarchical clustering schemes. *Psychometrika*, 32(3):241–254, 1967. ISSN 0033-3123.
- [72] Alain Jungo, Richard McKinley, Raphael Meier, Urspeter Knecht, Luis Vera, Julián Pérez-Beteta, David Molina-García, Víctor M Pérez-García, Roland Wiest, and Mauricio Reyes. Towards uncertainty-assisted brain tumor segmentation and survival prediction. In *International MICCAI Brainlesion Workshop*, pages 474–485. Springer.
- [73] Jayashree Kalpathy-Cramer, John Blake Freymann, Justin Stephen Kirby, Paul Eugene Kinahan, and Fred William Prior. Quantitative imaging network: data sharing and competitive algorithm-validation leveraging the cancer imaging archive. *Translational oncology*, 7(1):147–152, 2014. ISSN 1936-5233.
- [74] Konstantinos Kamnitsas, Wenjia Bai, Enzo Ferrante, Steven McDonagh, Matthew Sinclair, Nick Pawlowski, Martin Rajchl, Matthew Lee, Bernhard Kainz, and Daniel Rueckert. Ensembles of multiple models and architectures for robust brain tumour segmentation. In *International MICCAI Brainlesion Workshop*, pages 450–462. Springer.
- [75] Konstantinos Kamnitsas, Christian Ledig, Virginia FJ Newcombe, Joanna P Simpson, Andrew D Kane, David K Menon, Daniel Rueckert, and Ben Glocker. Efficient multi-scale 3d cnn with fully connected crf for accurate brain lesion segmentation. *Medical image analysis*, 36:61–78, 2017. ISSN 1361-8415.
- [76] Tapas Kanungo, David M Mount, Nathan S Netanyahu, Christine D Piatko, Ruth Silverman, and Angela Y Wu. An efficient k-means clustering algorithm: Analysis and implementation. *IEEE transactions on pattern analysis and machine intelligence*, 24(7):881–892, 2002. ISSN 0162-8828.
- [77] Hikmat Khan, Pir Masoom Shah, Munam Ali Shah, Saif ul Islam, and Joel JPC Rodrigues. Cascading handcrafted features and convolutional neural network for iot-enabled brain tumor segmentation. *Computer Communications*, 153:196–207, 2020. ISSN 0140-3664.
- [78] Jonghoon Kim, Seong-Yoon Ryu, Seung-Hak Lee, Ho Yun Lee, and Hyunjin Park. Clustering approach to identify intratumour heterogeneity combining fdg pet and diffusion-weighted mri in lung adenocarcinoma. *European radiology*, 29(1):468–475, 2019. ISSN 0938-7994.
- [79] Ron Kohavi and George H John. Wrappers for feature subset selection. *Artificial intelligence*, 97(1-2):273–324, 1997. ISSN 0004-3702.
- [80] Xiangmao Kong, Guoxia Sun, Qiang Wu, Ju Liu, and Fengming Lin. Hybrid pyramid u-net model for brain tumor segmentation. In *International conference on intelligent information processing*, pages 346–355. Springer.
- [81] Eleftherios Kontopodis, Georgios C Manikis, Iraklis Skepasianos, K Tzagkarakis, Katerina Niki-foraki, Georgios Z Papadakis, Thomas G Maris, Efrosini Papadaki, Apostolos Karantanas, and Kostas Marias. Dce-mri radiomics features for predicting breast cancer neoadjuvant therapy response. In *2018 IEEE International Conference on Imaging Systems and Techniques (IST)*, pages 1–6. IEEE. ISBN 1538666286.
- [82] Alex Krizhevsky, Ilya Sutskever, and Geoffrey E Hinton. Imagenet classification with deep convolutional neural networks. In *Advances in neural information processing systems*, pages 1097–1105.

- [83] Miron B Kurşa and Witold R Rudnicki. Feature selection with the boruta package. *J Stat Softw*, 36(11):1–13, 2010.
- [84] Jiangwei Lao, Yinsheng Chen, Zhi-Cheng Li, Qihua Li, Ji Zhang, Jing Liu, and Guangtao Zhai. A deep learning-based radiomics model for prediction of survival in glioblastoma multiforme. *Scientific reports*, 7(1):1–8, 2017. ISSN 2045-2322.
- [85] Floriane Legot, Florent Tixier, Minea Hadzic, Thomas Pinto-Leite, Christelle Gallais, Rémy Perdrisot, Xavier Dufour, and Catherine Cheze-Le-Rest. Use of baseline 18f-fdg pet scan to identify initial sub-volumes with local failure after concomitant radio-chemotherapy in head and neck cancer. *Oncotarget*, 9(31):21811, 2018.
- [86] Yang Lei, Xiangyang Tang, Kristin Higgins, Jolinta Lin, Jiwoong Jeong, Tian Liu, Anees Dhabaan, Tonghe Wang, Xue Dong, and Robert Press. Learning-based cbct correction using alternating random forest based on auto-context model. *Medical physics*, 46(2):601–618, 2019. ISSN 2473-4209.
- [87] Chao Li, Shuo Wang, Jiun-Lin Yan, Rory J Piper, Hongxiang Liu, Turid Torheim, Hyunjin Kim, Jingjing Zou, Natalie R Boonzaier, and Rohitashwa Sinha. Intratumoral heterogeneity of glioblastoma infiltration revealed by joint histogram analysis of diffusion tensor imaging. *Neurosurgery*, 85(4):524–534, 2019. ISSN 0148-396X.
- [88] Haichun Li, Ao Li, and Minghui Wang. A novel end-to-end brain tumor segmentation method using improved fully convolutional networks. *Computers in biology and medicine*, 108:150–160, 2019. ISSN 0010-4825.
- [89] Zhi-Cheng Li, Hongmin Bai, Qiuchang Sun, Yuanshen Zhao, Yanchun Lv, Jian Zhou, Chaofeng Liang, Yinsheng Chen, Dong Liang, and Hairong Zheng. Multiregional radiomics profiling from multiparametric mri: Identifying an imaging predictor of idh1 mutation status in glioblastoma. *Cancer medicine*, 7(12):5999–6009, 2018. ISSN 2045-7634.
- [90] Andy Liaw and Matthew Wiener. Classification and regression by randomforest. *R news*, 2(3):18–22, 2002. ISSN 1609-3631.
- [91] Fengming Lin, Ju Liu, Qiang Wu, Xiangmao Kong, Waliullah Khan, Wei Shi, and Enshuai Pang. Fmnet: Feature mining networks for brain tumor segmentation. In *2019 IEEE 31st International Conference on Tools with Artificial Intelligence (ICTAI)*, pages 555–560. IEEE. ISBN 1728137985.
- [92] Fengming Lin, Qiang Wu, Ju Liu, Dawei Wang, and Xiangmao Kong. Path aggregation u-net model for brain tumor segmentation. *Multimedia Tools and Applications*, pages 1–14, 2020. ISSN 1573-7721.
- [93] Mingquan Lin, Weifu Chen, Mingbo Zhao, Eli Gibson, Matthew Bastian-Jordan, Derek W Cool, Zahra Kassam, Huageng Liang, Tommy WS Chow, and Aaron D Ward. Prostate lesion delineation from multiparametric magnetic resonance imaging based on locality alignment discriminant analysis. *Medical physics*, 45(10):4607–4618, 2018. ISSN 0094-2405.
- [94] Mingquan Lin, He Cui, Weifu Chen, Arna van Engelen, Marleen de Bruijne, M Reza Azarpazhooh, Seyed Mojtaba Sohrevardi, J David Spence, and Bernard Chiu. Longitudinal assessment of carotid plaque texture in three-dimensional ultrasound images based on semi-supervised graph-based dimensionality reduction and feature selection. *Computers in Biology and Medicine*, 116:103586, 2020. ISSN 0010-4825.
- [95] Jinping Liu, Hui Liu, Zhaohui Tang, Weihua Gui, Tianyu Ma, Subo Gong, Quanquan Gao, Yongfang Xie, and Jean Paul Niyoyita. iouc-3dsfncn: Segmentation of brain tumors via iou constraint 3d symmetric full convolution network with multimodal auto-context. *Scientific Reports*, 10(1):1–15, 2020. ISSN 2045-2322.
- [96] Jonathan Long, Evan Shelhamer, and Trevor Darrell. Fully convolutional networks for semantic segmentation. In *Proceedings of the IEEE conference on computer vision and pattern recognition*, pages 3431–3440.

- [97] David N Louis, Arie Perry, Guido Reifenberger, Andreas Von Deimling, Dominique Figarella-Branger, Webster K Cavenee, Hiroko Ohgaki, Otmar D Wiestler, Paul Kleihues, and David W Ellison. The 2016 world health organization classification of tumors of the central nervous system: a summary. *Acta neuropathologica*, 131(6):803–820, 2016. ISSN 0001-6322.
- [98] Hecheng Lu and Jiandong Yin. Texture analysis of breast dce-mri based on intratumoral subregions for predicting her2+ status. *Frontiers in Oncology*, 10:543, 2020. ISSN 2234-943X.
- [99] François Lucia, Omar Miranda, Ronan Abgral, Vincent Bourbonne, Gurvan Dissaux, Olivier Pradier, Mathieu Hatt, and Ulrike Schick. Use of baseline 18f-fdg pet/ct to identify initial subvolumes associated with local failure after concomitant chemoradiotherapy in locally advanced cervical cancer. *Frontiers in Oncology*, 10:678, 2020. ISSN 2234-943X.
- [100] David Mattes, David R Haynor, Hubert Vesselle, Thomas K Lewellen, and William Eubank. Pet-ct image registration in the chest using free-form deformations. *IEEE transactions on medical imaging*, 22(1):120–128, 2003. ISSN 0278-0062.
- [101] Richard McKinley, Raphael Meier, and Roland Wiest. Ensembles of densely-connected cnns with label-uncertainty for brain tumor segmentation. In *International MICCAI Brainlesion Workshop*, pages 456–465. Springer, .
- [102] Richard McKinley, Michael Rebsamen, Raphael Meier, and Roland Wiest. Triplanar ensemble of 3d-to-2d cnns with label-uncertainty for brain tumor segmentation. In *International MICCAI Brainlesion Workshop*, pages 379–387. Springer, .
- [103] Bjoern H Menze, Andras Jakab, Stefan Bauer, Jayashree Kalpathy-Cramer, Keyvan Farahani, Justin Kirby, Yuliya Burren, Nicole Porz, Johannes Slotboom, and Roland Wiest. The multimodal brain tumor image segmentation benchmark (brats). *IEEE transactions on medical imaging*, 34(10):1993–2024, 2014. ISSN 0278-0062.
- [104] Sean Miller, Pin Li, Matthew Schipper, Larry Junck, Morand Piert, Theodore S Lawrence, Christina Tsien, Yue Cao, and Michelle M Kim. Metabolic tumor volume response assessment using (11)c-methionine positron emission tomography identifies glioblastoma tumor subregions that predict progression better than baseline or anatomic magnetic resonance imaging alone. *Advances in Radiation Oncology*, 5(1):53–61, 2020. ISSN 2452-1094.
- [105] Pawel Mlynarski, Hervé Delingette, Antonio Criminisi, and Nicholas Ayache. 3d convolutional neural networks for tumor segmentation using long-range 2d context. *Computerized Medical Imaging and Graphics*, 73:60–72, 2019. ISSN 0895-6111.
- [106] Andriy Myronenko. 3d mri brain tumor segmentation using autoencoder regularization. In *International MICCAI Brainlesion Workshop*, pages 311–320. Springer.
- [107] Shubhangi Nema, Akshay Dudhane, Subrahmanyam Murala, and Srivatsava Naidu. Rescuenet: An unpaired gan for brain tumor segmentation. *Biomedical Signal Processing and Control*, 55:101641, 2020. ISSN 1746-8094.
- [108] Sumihito Nobusawa, Takuya Watanabe, Paul Kleihues, and Hiroko Ohgaki. Idh1 mutations as molecular signature and predictive factor of secondary glioblastomas. *Clinical Cancer Research*, 15(19):6002–6007, 2009. ISSN 1078-0432.
- [109] James PB O’Connor, Chris J Rose, John C Waterton, Richard AD Carano, Geoff JM Parker, and Alan Jackson. Imaging intratumor heterogeneity: role in therapy response, resistance, and clinical outcome. *Clinical Cancer Research*, 21(2):249–257, 2015. ISSN 1078-0432.
- [110] Ozan Oktay, Jo Schlemper, Loic Le Folgoc, Matthew Lee, Mattias Heinrich, Kazunari Misawa, Kensaku Mori, Steven McDonagh, Nils Y Hammerla, and Bernhard Kainz. Attention u-net: Learning where to look for the pancreas. *arXiv preprint arXiv:1804.03999*, 2018.
- [111] Alexander FI Osman. A multi-parametric mri-based radiomics signature and a practical ml model for stratifying glioblastoma patients based on survival toward precision oncology. *Frontiers in Computational Neuroscience*, 13, 2019.

- [112] Brian O’Sullivan, Shao Hui Huang, Jie Su, Adam S Garden, Erich M Sturgis, Kristina Dahlstrom, Nancy Lee, Nadeem Riaz, Xin Pei, and Shlomo A Koyfman. Development and validation of a staging system for hpv-related oropharyngeal cancer by the international collaboration on oropharyngeal cancer network for staging (icon-s): a multicentre cohort study. *The Lancet Oncology*, 17(4):440–451, 2016. ISSN 1470-2045.
- [113] Nobuyuki Otsu. A threshold selection method from gray-level histograms. *IEEE transactions on systems, man, and cybernetics*, 9(1):62–66, 1979. ISSN 0018-9472.
- [114] Sinno Jialin Pan and Qiang Yang. A survey on transfer learning. *IEEE transactions on knowledge and data engineering*. 22(10): 1345, 1359, 2010.
- [115] D Williams Parsons, Siân Jones, Xiaosong Zhang, Jimmy Cheng-Ho Lin, Rebecca J Leary, Philipp Angenendt, Parminder Mankoo, Hannah Carter, I-Mei Siu, and Gary L Gallia. An integrated genomic analysis of human glioblastoma multiforme. *science*, 321(5897):1807–1812, 2008. ISSN 0036-8075.
- [116] A Pena, HAL Green, TA Carpenter, SJ Price, JD Pickard, and JH Gillard. Enhanced visualization and quantification of magnetic resonance diffusion tensor imaging using the p: q tensor decomposition. *The British journal of radiology*, 79(938):101–109, 2006. ISSN 0007-1285.
- [117] Sérgio Pereira, Adriano Pinto, Victor Alves, and Carlos A Silva. Brain tumor segmentation using convolutional neural networks in mri images. *IEEE transactions on medical imaging*, 35(5):1240–1251, 2016. ISSN 0278-0062.
- [118] Stephen J Price, Kieren Allinson, Hongxiang Liu, Natalie R Boonzaier, Jiun-Lin Yan, Victoria C Lupson, and Timothy J Larkin. Less invasive phenotype found in isocitrate dehydrogenase–mutated glioblastomas than in isocitrate dehydrogenase wild-type glioblastomas: a diffusion-tensor imaging study. *Radiology*, 283(1):215–221, 2017. ISSN 0033-8419.
- [119] Elodie Puybareau, Guillaume Tochon, Joseph Chazalon, and Jonathan Fabrizio. Segmentation of gliomas and prediction of patient overall survival: a simple and fast procedure. In *International MICCAI Brainlesion Workshop*, pages 199–209. Springer.
- [120] Kehan Qi, Hao Yang, Cheng Li, Zaiyi Liu, Meiyun Wang, Qiegen Liu, and Shanshan Wang. X-net: Brain stroke lesion segmentation based on depthwise separable convolution and long-range dependencies. In *International Conference on Medical Image Computing and Computer-Assisted Intervention*, pages 247–255. Springer.
- [121] RC Quinlan. 4.5: Programs for machine learning morgan kaufmann publishers inc. *San Francisco, USA*, 1993.
- [122] Asra Rafi, Junaid Ali, Tahir Akram, Kiran Fiaz, Ahmad Raza Shahid, Basit Raza, and Tahir Mustafa Madni. U-net based glioblastoma segmentation with patient’s overall survival prediction. In *International Symposium on Intelligent Computing Systems*, pages 22–32. Springer.
- [123] Farheen Ramzan, Muhammad Usman Ghani Khan, Sajid Iqbal, Tanzila Saba, and Amjad Rehman. Volumetric segmentation of brain regions from mri scans using 3d convolutional neural networks. *IEEE Access*, 8:103697–103709, 2020. ISSN 2169-3536.
- [124] Max Rohde, Anne L Nielsen, Manan Pareek, Jørgen Johansen, Jens A Sørensen, Anabel Diaz, Mie K Nielsen, Janus M Christiansen, Jon T Asmussen, and Nina Nguyen. Pet/ct versus standard imaging for prediction of survival in patients with recurrent head and neck squamous cell carcinoma. *Journal of Nuclear Medicine*, 60(5):592–599, 2019. ISSN 0161-5505.
- [125] Olaf Ronneberger, Philipp Fischer, and Thomas Brox. U-net: Convolutional networks for biomedical image segmentation. In *International Conference on Medical image computing and computer-assisted intervention*, pages 234–241. Springer.
- [126] Frank Rosenblatt. Principles of neurodynamics. perceptrons and the theory of brain mechanisms. Report, Cornell Aeronautical Lab Inc Buffalo NY, 1961.

- [127] Marc Sanson, Yannick Marie, Sophie Paris, Ahmed Idbaih, Julien Laffaire, François Ducray, Soufi-ane El Hallani, Blandine Boisselier, Karima Mokhtari, and Khe Hoang-Xuan. Isocitrate dehydrogenase 1 codon 132 mutation is an important prognostic biomarker in gliomas. *J Clin Oncol*, 27(25):4150–4154, 2009.
- [128] Rachida Saouli, Mohamed Akil, and Rostom Kachouri. Fully automatic brain tumor segmentation using end-to-end incremental deep neural networks in mri images. *Computer methods and programs in biomedicine*, 166:39–49, 2018. ISSN 0169-2607.
- [129] P Seow, MT Win, JHD Wong, NA Abdullah, and N Ramli. Segmentation of solid subregion of high grade gliomas in mri images based on active contour model (acm). In *Journal of Physics: Conference Series*, volume 694, pages 1–12.
- [130] Muhammad Irfan Sharif, Jian Ping Li, Muhammad Attique Khan, and Muhammad Asim Saleem. Active deep neural network features selection for segmentation and recognition of brain tumors using mri images. *Pattern Recognition Letters*, 129:181–189, 2020. ISSN 0167-8655.
- [131] Zeina A Shboul, Lasitha Vidyaratne, Mahbubul Alam, and Khan M Iftekharuddin. Glioblastoma and survival prediction. In *International MICCAI Brainlesion Workshop*, pages 358–368. Springer.
- [132] Zahra Sobhaninia, Safiyeh Rezaei, Alireza Noroozi, Mehdi Ahmadi, Hamidreza Zarrabi, Nader Karimi, Ali Emami, and Shadrokh Samavi. Brain tumor segmentation using deep learning by type specific sorting of images. *arXiv preprint arXiv:1809.07786*, 2018.
- [133] Qi SongTao, Yu Lei, Gui Si, Ding YanQing, Han HuiXia, Zhang XueLin, Wu LanXiao, and Yao Fei. Idh mutations predict longer survival and response to temozolomide in secondary glioblastoma. *Cancer science*, 103(2):269–273, 2012. ISSN 1347-9032.
- [134] B Srinivas and Gottapu Sasibhushana Rao. Segmentation of multi-modal mri brain tumor sub-regions using deep learning.
- [135] Li Sun, Songtao Zhang, and Lin Luo. Tumor segmentation and survival prediction in glioma with deep learning. In *International MICCAI Brainlesion Workshop*, pages 83–93. Springer.
- [136] Muyi Sun, Kaiyi Liang, Wenbao Zhang, Qing Chang, and Xiaoguang Zhou. Non-local attention and densely-connected convolutional neural networks for malignancy suspiciousness classification of gastric ulcer. *IEEE Access*, 8:15812–15822, 2020. ISSN 2169-3536.
- [137] Haochen Tan, Huimin Shi, Mingquan Lin, J David Spence, Kwok-Leung Chan, and Bernard Chiu. Vessel wall segmentation of common carotid artery via multi-branch light network. In *Medical Imaging 2020: Image Processing*, volume 11313, page 1131311. International Society for Optics and Photonics.
- [138] Robert Tibshirani. Regression shrinkage and selection via the lasso. *Journal of the Royal Statistical Society: Series B (Methodological)*, 58(1):267–288, 1996. ISSN 0035-9246.
- [139] Turid Torheim, Aurora R Groendahl, Erlend KF Andersen, Heidi Lyng, Eirik Malinen, Knut Kvaal, and Cecilia M Futsaether. Cluster analysis of dynamic contrast enhanced mri reveals tumor subregions related to locoregional relapse for cervical cancer patients. *Acta oncologica*, 55(11):1294–1298, 2016. ISSN 0284-186X.
- [140] A Vamvakas, SC Williams, K Theodorou, E Kapsalaki, K Fountas, C Kappas, K Vassiou, and I Tsougos. Imaging biomarker analysis of advanced multiparametric mri for glioma grading. *Physica Medica*, 60:188–198, 2019. ISSN 1120-1797.
- [141] Petar Veličković, Guillem Cucurull, Arantxa Casanova, Adriana Romero, Pietro Lio, and Yoshua Bengio. Graph attention networks. *arXiv preprint arXiv:1710.10903*, 2017.
- [142] Fei Wang, Mengqing Jiang, Chen Qian, Shuo Yang, Cheng Li, Honggang Zhang, Xiaogang Wang, and Xiaou Tang. Residual attention network for image classification. In *Proceedings of the IEEE conference on computer vision and pattern recognition*, pages 3156–3164, .
- [143] Feifan Wang, Runzhou Jiang, Liqin Zheng, Chun Meng, and Bharat Biswal. 3d u-net based brain tumor segmentation and survival days prediction. In *International MICCAI Brainlesion Workshop*, pages 131–141. Springer, .

- [144] Guotai Wang, Wenqi Li, Sébastien Ourselin, and Tom Vercauteren. Automatic brain tumor segmentation using cascaded anisotropic convolutional neural networks. In *International MICCAI brainlesion workshop*, pages 178–190. Springer, .
- [145] Guotai Wang, Wenqi Li, Tom Vercauteren, and Sebastien Ourselin. Automatic brain tumor segmentation based on cascaded convolutional neural networks with uncertainty estimation. *Frontiers in computational neuroscience*, 13:56, 2019. ISSN 1662-5188.
- [146] Hesheng Wang, Reza Farjam, Mary Feng, Hero Hussain, Randall K Ten Haken, Theodore S Lawrence, and Yue Cao. Arterial perfusion imaging–defined subvolume of intrahepatic cancer. *International Journal of Radiation Oncology\* Biology\* Physics*, 89(1):167–174, 2014. ISSN 0360-3016.
- [147] Liansheng Wang, Shuxin Wang, Rongzhen Chen, Xiaobo Qu, Yiping Chen, Shaohui Huang, and Changhua Liu. Nested dilation networks for brain tumor segmentation based on magnetic resonance imaging. *Frontiers in Neuroscience*, 13:285, 2019. ISSN 1662-453X.
- [148] Peng Wang, Aron Popovtzer, Avraham Eisbruch, and Yue Cao. An approach to identify, from dce mri, significant subvolumes of tumors related to outcomes in advanced head-and-neck cancer a. *Medical physics*, 39(8):5277–5285, 2012. ISSN 0094-2405.
- [149] Shuo Wang, Chengliang Dai, Yuanhan Mo, Elsa Angelini, Yike Guo, and Wenjia Bai. Automatic brain tumour segmentation and biophysics-guided survival prediction. In *International MICCAI Brainlesion Workshop*, pages 61–72. Springer, .
- [150] Wenguan Wang, Shuyang Zhao, Jianbing Shen, Steven CH Hoi, and Ali Borji. Salient object detection with pyramid attention and salient edges. In *Proceedings of the IEEE Conference on Computer Vision and Pattern Recognition*, pages 1448–1457, .
- [151] Leon Weninger, Oliver Rippel, Simon Koppers, and Dorit Merhof. Segmentation of brain tumors and patient survival prediction: methods for the brats 2018 challenge. In *International MICCAI Brainlesion Workshop*, pages 3–12. Springer.
- [152] Svante Wold, Kim Esbensen, and Paul Geladi. Principal component analysis. *Chemometrics and intelligent laboratory systems*, 2(1-3):37–52, 1987. ISSN 0169-7439.
- [153] Jia Wu, Todd Aguilera, David Shultz, Madhu Gudur, Daniel L Rubin, Billy W Loo Jr, Maximilian Diehn, and Ruijiang Li. Early-stage non–small cell lung cancer: quantitative imaging characteristics of 18f fluorodeoxyglucose pet/ct allow prediction of distant metastasis. *Radiology*, 281(1):270–278, 2016. ISSN 0033-8419.
- [154] Jia Wu, Michael F Gensheimer, Xinzhe Dong, Daniel L Rubin, Sandy Napel, Maximilian Diehn, Billy W Loo Jr, and Ruijiang Li. Robust intratumor partitioning to identify high-risk subregions in lung cancer: a pilot study. *International Journal of Radiation Oncology\* Biology\* Physics*, 95(5):1504–1512, 2016. ISSN 0360-3016.
- [155] Jia Wu, Guohong Cao, Xiaoli Sun, Juheon Lee, Daniel L Rubin, Sandy Napel, Allison W Kurian, Bruce L Daniel, and Ruijiang Li. Intratumoral spatial heterogeneity at perfusion mr imaging predicts recurrence-free survival in locally advanced breast cancer treated with neoadjuvant chemotherapy. *Radiology*, 288(1):26–35, 2018. ISSN 0033-8419.
- [156] Jia Wu, Michael F Gensheimer, Nasha Zhang, Meiying Guo, Rachel Liang, Carrie Zhang, Nancy Fischbein, Erqi L Pollom, Beth Beadle, and Quynh-Thu Le. Tumor subregion evolution-based imaging features to assess early response and predict prognosis in oropharyngeal cancer. *Journal of Nuclear Medicine*, 61(3):327–336, 2020. ISSN 0161-5505.
- [157] Congying Xie, Pengfei Yang, Xuebang Zhang, Lei Xu, Xiaoju Wang, Xiadong Li, Luhan Zhang, Ruifei Xie, Ling Yang, and Zhao Jing. Sub-region based radiomics analysis for survival prediction in oesophageal tumours treated by definitive concurrent chemoradiotherapy. *EBioMedicine*, 44:289–297, 2019. ISSN 2352-3964.

- [158] Hui Xu, Wenbing Lv, Hui Feng, Dongyang Du, Qingyu Yuan, Quanshi Wang, Zhenhui Dai, Wei Yang, Qianjin Feng, and Jianhua Ma. Subregional radiomics analysis of pet/ct imaging with intra-tumor partitioning: application to prognosis for nasopharyngeal carcinoma. *Molecular Imaging and Biology*, pages 1–13, 2019. ISSN 1860-2002.
- [159] Qian Yang, Lihua Li, Juan Zhang, Guoliang Shao, Chengjie Zhang, and Bin Zheng. Computer-aided diagnosis of breast dce-mri images using bilateral asymmetry of contrast enhancement between two breasts. *Journal of digital imaging*, 27(1):152–160, 2014. ISSN 0897-1889.
- [160] T Yang, Y Ou, and T Huang. Automatic segmentation of brain tumor from mr images using segnet: selection of training data sets. In *Proc. 6th MICCAI BraTS Challenge*, pages 309–312.
- [161] Hang Zhang, Han Zhang, Chenguang Wang, and Junyuan Xie. Co-occurrent features in semantic segmentation. In *Proceedings of the IEEE Conference on Computer Vision and Pattern Recognition*, pages 548–557.
- [162] Jianpeng Zhang, Yutong Xie, Yong Xia, and Chunhua Shen. Attention residual learning for skin lesion classification. *IEEE transactions on medical imaging*, 38(9):2092–2103, 2019. ISSN 0278-0062.
- [163] Jianxin Zhang, Zongkang Jiang, Jing Dong, Yaqing Hou, and Bin Liu. Attention gate resu-net for automatic mri brain tumor segmentation. *IEEE Access*, 8:58533–58545, 2020. ISSN 2169-3536.
- [164] Xi Zhang, Hongbing Lu, Qiang Tian, Na Feng, Lulu Yin, Xiaopan Xu, Peng Du, and Yang Liu. A radiomics nomogram based on multiparametric mri might stratify glioblastoma patients according to survival. *European radiology*, 29(10):5528–5538, 2019. ISSN 0938-7994.
- [165] Yongyue Zhang, Michael Brady, and Stephen Smith. Segmentation of brain mr images through a hidden markov random field model and the expectation-maximization algorithm. *IEEE transactions on medical imaging*, 20(1):45–57, 2001. ISSN 0278-0062.
- [166] Yue Zhang, Xianrui Li, Mingquan Lin, Bernard Chiu, and Mingbo Zhao. Deep-recursive residual network for image semantic segmentation. *Neural Computing and Applications*, pages 1–13, 2020. ISSN 1433-3058.
- [167] Yupei Zhang, Yang Lei, Richard LJ Qiu, Tonghe Wang, Hesheng Wang, Ashesh B Jani, Walter J Curran, Pretesh Patel, Tian Liu, and Xiaofeng Yang. Multi-needle localization with attention u-net in us-guided hdr prostate brachytherapy. *Medical Physics*, 2020. ISSN 0094-2405.
- [168] Xiaomei Zhao, Yihong Wu, Guidong Song, Zhenye Li, Yazhuo Zhang, and Yong Fan. A deep learning model integrating fcnn and crfs for brain tumor segmentation. *Medical image analysis*, 43:98–111, 2018. ISSN 1361-8415.
- [169] Yuan-Xing Zhao, Yan-Ming Zhang, and Cheng-Lin Liu. Bag of tricks for 3d mri brain tumor segmentation. In *International MICCAI Brainlesion Workshop*, pages 210–220. Springer.
- [170] Boran Zhou, Brian J Bartholmai, Sanjay Kalra, and Xiaoming Zhang. Predicting lung mass density of patients with interstitial lung disease and healthy subjects using deep neural network and lung ultrasound surface wave elastography. *Journal of the Mechanical Behavior of Biomedical Materials*, 104:103682, 2020. ISSN 1751-6161.
- [171] Chenhong Zhou, Shengcong Chen, Changxing Ding, and Dacheng Tao. Learning contextual and attentive information for brain tumor segmentation. In *International MICCAI Brainlesion Workshop*, pages 497–507. Springer.
- [172] Chenhong Zhou, Changxing Ding, Xinchao Wang, Zhentai Lu, and Dacheng Tao. One-pass multi-task networks with cross-task guided attention for brain tumor segmentation. *IEEE Transactions on Image Processing*, 29:4516–4529, 2020. ISSN 1057-7149.
- [173] Lei Zhou and Weiyufeng Wei. Dic: Deep image clustering for unsupervised image segmentation. *IEEE Access*, 8:34481–34491, 2020. ISSN 2169-3536.
- [174] Mu Zhou, Baishali Chaudhury, Lawrence O Hall, Dmitry B Goldgof, Robert J Gillies, and Robert A Gatenby. Identifying spatial imaging biomarkers of glioblastoma multiforme for survival group prediction. *Journal of Magnetic Resonance Imaging*, 46(1):115–123, 2017. ISSN 1053-1807.